Mar. 11, 2005
prepared for *J. Phys. Chem. A*

Databases for Transition Element Bonding: Metal–Metal Bond Energies and Bond Lengths and Their Use to Test Hybrid, Hybrid Meta, and Meta Density Functionals and Generalized Gradient Approximations

Nathan E. Schultz, Yan Zhao, and Donald G. Truhlar*

Department of Chemistry and Supercomputing Institute, University of Minnesota, 207 Pleasant Street Southeast, Minneapolis MN 55455-0431, USA

We propose a data set of bond lengths for 8 selected transition metal dimers (Ag_2, Cr_2, Cu_2, CuAg, Mo_2, Ni_2, V_2, and Zr_2) and another data set containing their atomization energies and the atomization energies of ZrV, and we use these for testing density functional theory. The molecules chosen for the test sets were selected on the basis of the expected reliability of the data and their ability to constitute a diverse and representative set of transition element bond types while keeping the data sets small enough to allow for efficient testing of a large number of computational methods against a very reliable subset of experimental data. In this paper we test 42 different functionals: 2 local spin density approximation (LSDA) functionals, 12 generalized gradient approximation (GGA) methods, 13 hybrid GGAs, 7 meta GGA methods, and 8 hybrid meta GGAs. We find that GGA density functionals are more accurate for the atomization energies of pure transition metal systems than are their meta, hybrid, or hybrid meta analogs. We find that the errors for atomization energies and bond lengths are not as large if we limit ourselves to dimers with small amounts of multireference character. We also demonstrate the effects of increasing the fraction of Hartree–Fock exchange in multireference systems by computing the potential energy curve for Cr_2 and Mo_2 with multiple methods. We also find that BLYP is the most accurate functional for bond energies and is reasonably accurate for bond lengths. The methods that work well for transition metal bonds are found to be quite different than those that work well for organic and other main group chemistry.

I. Introduction

Density functional theory[1] (DFT) has become a popular method for calculating a variety of molecular properties. It may be fair to say that the popularity of DFT methods has been motivated by their affordability, that is by their promise, not yet fully achieved, of high accuracy at relatively low cost. When employing atom-centered basis functions and conventional algorithms, the computational cost of DFT calculations scales as N^4, where N is the number of basis functions, whereas accurate correlated wave function theory (WFT) methods scale as N^7 or worse.[2] The scaling can be improved in both approaches by using other algorithms, but DFT is still expected to become more and more favorable compared to WFT methods as system size increases. This has generated a considerable amount of activity in optimizing and testing DFT with various functionals. For applications to small molecules composed of main group elements, hybrid DFT, in which the functional contains a component of Hartree–Fock exchange, has been shown to be superior to non-hybrid DFT for both atomization energies[3] and barrier heights.[4,5] Nevertheless the most accurate DFT methods also include density-based exchange, partly for consistency[6] with imperfect density-based dynamical correlation functionals and partly because density-based exchange includes important effects usually described in WFT language as static (or internal or left-right or non-dynamical[2]) correlation.[2,7-10]

The large numbers of nearly degenerate electronic states in transition elements are associated with very important static correlation effects, and the treatment of these effects by well balanced correlated WFT methods requires a large amount of multireference character, which is not typical of closed-shell molecules formed from main group elements.[11] In this context, density-based exchange functionals may provide a more

theoretically justified way to treat transition metals than post-Hartree–Fock WFT methods and not just a cost effective alternative to WFT.[10]

DFT methods may be classified in various ways. In this paper we classify the various approaches in terms of the kind of functionals they employ. (i) Local spin density approximation (LSDA) functionals depend only on the up-spin and down-spin electron density. (ii) Generalized gradient approximation (GGA) functionals depend not only on the density but also on the magnitude of the gradient of the density. (iii) Hybrid DFT functionals combine GGAs with Hartree–Fock exchange and replace the Kohn–Sham operators with hybrid Fock–Kohn–Sham operators. (iv) Meta DFT functionals combine GGAs with additional functionals that are called meta functionals and that depend on kinetic energy density. (v) Hybrid meta DFT functionals combine GGAs, meta functionals, and Hartree–Fock exchange. Both Hartree–Fock exchange and meta functionals involve Kohn–Sham or Fock–Kohn–Sham orbitals, but these orbitals are functionals of the density and hence all five varieties of DFT considered here can be written in terms of energy functionals of the density.

It is important to systematically study the accuracy of the available functionals for transition metals. There have been a very large number of studies that have benchmarked the accuracy of DFT methods for main group molecules, and there are an increasing number of DFT studies[12-16] designed to test DFT for bonding in transition metal dimers. But the studies of transition metal bonding are not completely satisfactory for four reasons: (1) Only 5-8 functionals are tested in each paper; thus one is not certain that the absolutely best functional has been identified for transition metals. (2) Different papers test different functionals, which makes it difficult to reconcile the conclusions that one

draws from one paper with the conclusions that one draws from another. For example, Barden *et al.*[12] studied all of the 3*d* homonuclear dimers except Zn with 5 methods (3 hybrid and 2 non-hybrid methods), Gustev and Bauschlicher[17] studied all of the homonuclear 3*d* metal diatomics with 6 non-hybrid functionals, and Wu[16] studied the 4*d* homonuclear transition metals with 6 hybrid and 2 non-hybrid functionals. However, those studies had only two functionals in common, and one of the functionals recommended by Gustev and Bauschlicher (BPW91)[18,19] was not present in the other two studies. Furthermore, Wu indicates that using hybrid functionals may be appropriate for some properties, but hybrid functionals are not studied by Gustev and Bauschlicher, and Barden *et al.* recommend against the use of hybrid functionals. (3) The functionals are often tested against all of the 3*d* or 4*d* transition metal dimers. This strategy may, at first glance, seem like the most thorough way to study the accuracy of transition metals, but the experimental data is not uniformly reliable for the entire series of transition metal dimers. Thus, it is more appropriate to have a small and representative test set from which uncertain pieces of data are excluded. (4) It is not always clear that previous workers have identified the lowest-energy electronic states of the atoms and dimers for each DFT method tested, and a failure to do this could skew the conclusions.

II. Databases

The TMBL8/05 database consists of the bond lengths for eight dimers: Ag_2, Cr_2, Cu_2, CuAg, Mo_2, Ni_2, V_2, and Zr_2 and the TMAE9/05 database consists of the atomization energies of the dimers in TMBL8/05 plus the atomization energy of ZrV. The experimental data are summarized in Table 1. In both cases, we tried to achieve a balance between using only the most reliable data and having a representatively diverse

data set. In the latter, we have included *s*-bonded coinage dimers, *s*- and *d*-bonded early transition metal dimers, the extreme state-mixing case of Ni_2, the notoriously difficult cases of the weakly bound Cr_2 and strongly bound Mo_2, and heteronuclear dimers. Data that were purposefully excluded, despite their expected reliability, were cases such as Zn_2 and Mn_2, since they are best described as van der Waals molecules and might not provide useful insights into which methods are accurate for true metallic bonding.

We have relied mainly on the reviews of Lombardi and Davis[20] and Morse,[21] as well as our own reading of the original literature, for the homonuclear bond energies. The bond energy for Ni_2 comes from Pinegar *et al.*[22] and not the earlier value that was determined by Morse *et al.*[23] and reported by Lombardi and Davis[20] The equilibrium bond lengths (r_e) for Cr_2, Cu_2, Mo_2, and V_2 also come from Lombardi and Davis.[20] We have also included the bond length of Zr_2, which was first reported by Doverstål *et al.*[24] as an r_0 (the bond length in the first vibrational level), which we have converted to an r_e using the spectroscopic data from Doverstål *et al.*[24] and Lombardi and Davis[20] and equations 7.33 and 7.43 from Bernath's book.[25] We also note that the value for the Ni_2 bond length reported by Lombardi and Davis[20] is also for an r_0 (but is denoted as r_e in their paper). Therefore, we have also converted the Ni_2 bond length to an r_e using the same method as we did for Zr_2 and by taking the necessary spectroscopic constants from Lombardi and Davis.[20] We also take the r_e for Ag_2 from Morse[26] because Lombardi *et al.*[20] report an r_0. The heteronuclear data come from Bishea *et al.*[27], Langenberg and Morse[28], and Morse.[26]

The atomization energy (also called dissociation energy) is defined as the energy required to form infinitely separated atoms in their ground states. The experimental energies are dissociation energies at 0 K (often called D_0), and hence they include the zero-point energy in the molecules and spin-orbit effects in the atoms and molecules, whereas TMAE9/05 contains zero-point exclusive values (called D_e). To produce an experimental zero-point exclusive atomization energy, called D_e, for Ag_2, Cr_2, Cu_2, CuAg, Mo_2, Ni_2, V_2, and Zr_2, we have calculated the zero-point energies from ω_e and $x_e\omega_e$ (taken from Lombardi and Davis[20], Casey and Leopold,[29] and Morse[26]) and added them to the 0 K dissociation energies. To obtain D_e for the other molecule (ZrV) in TMAE9/05, the zero-point energy for ZrV was calculated with B3LYP/DZQ, where B3LYP and DZQ are explained in the next section, and scaled by a factor of 0.983. The scale factor was determined by a method[30] that consists of calculating the zero-point energies of several molecules and scaling them to reproduce (as well as possible in a least squares deviation sense) anharmonic zero-point energies. In the present case we used 20 molecules, namely Ag_2, Cu_2, CuAg, Mo_2, Ni_2, V_2, Zr_2, H_2, CH_4, NH_3, H_2O, HF, CO, N_2, F_2, C_2H_2, HCN, H_2CO, CO_2, and N_2O and calculated the zero-point energy with B3LYP/DZQ for the transition metals and B3LYP/6-31G(2d,p) for the main-group elements. The accurate zero-point energies for the main-group molecules in this list were taken from earlier work by Martin.[31]

III. Computational Methods

All of the calculations in this paper have been carried out with GAUSSIAN03.[32] As explained in Section I, we will test five different categories of DFT methods: LSDA, GGA, hybrid GGA, meta GGA, hybrid meta GGA methods. The LSDA functionals

depend only on the electron density. The GGA functionals depend explicitly on the gradient of the electron density as well as the density itself; hybrid GGA functionals depend on Hartree–Fock (HF) exchange as well as the electron density and its gradient. Meta GGA functionals depend on the electron density, its gradient, and the kinetic energy density. The hybrid meta GGA functionals depend on HF exchange, the electron density and its gradient, and the kinetic energy density. We will speak of LSDA, GGA, hybrid GGA, meta GGA, and hybrid meta GGA when specifically referring to one of the subsets, whereas the phrase "DFT methods" remains general and does not exclude hybrid, LSDA, or meta methods. The phrase "hybrid-methods" will refer to both hybrid GGA and hybrid meta GGA methods, and the "non-hybrid methods" will refer to LSDA, GGA, and meta GGA methods.

The LSDAs that we will assess are SWVN3[33,34] and SPWL.[33,35] The GGA methods that we will test are (in alphabetical order) BLYP,[18,36] BP86,[18,37] BPBE,[18,38] BPW91,[18,19] G96LYP,[36,39] HCTH[40] (also called HCTH407), mPWLYP,[36,41] mPWPBE,[38,41] mPWPW91,[41] OLYP,[36,42] PBE (PBE exchange with PBE correlation, also called PBEPBE),[38] and XLYP.[36,43] The hybrid GGA methods that we are using are B3LYP,[18,36,44] B3P96,[18,37] B3PW91,[3,18,19] B971-1,[40] B97-2,[45] B98,[46] BH&HLYP,[18,32,36] MPW1K,[19,41,47] mPW1PW91 (also called mPW0 and MPW25),[19,41] MPW3LYP,[36,41,48] O3LYP,[36,42,49] PBE1PBE (also called PBE0),[38,50] and X3LYP.[36,43] The meta DFT methods that we have tested are BB95,[18,51] mPWB95,[41] PBEKCIS,[38,52] TPSS (TPSS exchange with TPSS correlation, also called TPSSTPSS),[53] TPSSKCIS (TPSS exchange with KCIS correlation),[52,53] mPWKCIS,[41,52,54] and VSXC.[55] The hybrid meta GGA methods that we will study in this paper are B1B95,[18,51] BB1K,[18,48,51] MPW1B95,[41,48,51]

MPWB1K,[41,48,51] MPW1KCIS,[41,52,54] PBE1KCIS,[38,52,56] TPSS1KCIS,[19,52-54] and TPSSh (uses TPSS exchange and TPSS correlation).[53] The compositions of the functionals tested are summarized in Table 2, where they are listed in alphabetical order for the reader's convenience. Table 2 also gives *X*, which is the fraction of Hartree-Fock exchange.

Note that, consistently with the original papers, the mPW exchange functional is called MPW in combined functionals where one or more parameter was optimized in our group but mPW when used without such optimization (exception: MPW25 was developed by Adamo and Barone). Some of the notation is cumbersome, but we think it is better to use the well established conventions of the field than to try improve the names. Note also that the mPW functional was coded incorrectly in the original *Gaussian98* (through version a.11), but was corrected following Lynch *et al.*[57] for the mPW and MPW calculations reported here. Note also that the B1B95 functional was also incorrect in *Gaussian03* through version B01, but all B1B95 calculations reported here are correct (they have $X = 28$).

Although we are testing the functionals against small-molecule data, we expect our conclusions to be valid in a general way for metal–metal bonding in larger systems, such as megaclusters (roughly 10 – 40 atoms) or nanoparticles (40 – 10^6 atoms). For this reason we test the functionals both with effective core potentials (EC methods)[58,59] with moderate and large basis sets and with a large all-electron basis set. An EC method involves an analytic effective core potential, to mimic the presence of the core electrons, and a valence-electron basis set. The use of EC methods is motivated in two ways: (1) The computational efficiency is greatly increased, because only the chemically important

valence electrons are explicitly treated with basis functions, without a significant loss in accuracy. (2) Effective core potentials can be used to implicitly treat the relativistic effects,[60] which are largely confined to the core electrons and are important for transition metals in the second transition series (4*d*) and essential for those (5*d*, which are not considered here) in the third transition series.

We will test two levels of basis set, and we are denoting these as "DZQ" and "TZQ," which stands for double-zeta quality and triple-zeta quality. The DZQ basis set uses the relativistic EC method of Stevens *et al.,*[61-63] for both the 3*d* and 4*d* transition metals. The size of the valence electron basis set for the DZQ method is (8s8p6d)/[4s4p3d]. The TZQ basis set is defined as the all-electron (15s116d1f)/[10s7p4d1f] basis set[64-66] for the 3*d* transition metals, which is denoted 6-311+G* in GAUSSIAN03, and the DZQ basis set with additional *s*-, *p*-, and *d*-functions and *f*-polarization functions proposed by Langhoff *et al.*[67] for the 4*d* transition metals. The final size of the TZQ for Zr is (8s8p7d3f)/[4s4p4d3f] and (8s8p7d4f)/[4s4p4d3f] for Mo and Ag. This basis set for the 4*d* metals is not exactly the same as the one recommended by Langhoff *et al,*[67] specifically we do not include their most diffuse *s*- and *p*-functions, and we use the relativistic EC method of Stevens *et al.,*[61-63] whereas they used the relativistic EC method of Hay and Wadt.[68] The additional diffuse functions were deleted because we experienced a large number of convergence problems with the original basis set, and we found that our modifications did not change the results for the cases that did not have convergence problems. The TZQ basis set for the entire series of 4*d* transition metals (and—in fact—all basis sets used in this paper) can be obtained from http://comp.chem.umn.edu/basissets/basis.cgi.

In one section we will give a limited number of results with a basis that we will call TZQ+*g*. In this basis set, we will add a set of *g*-polarization functions to the TZQ basis set for the 4*d* elements. The sets of *g*-functions were taken from Eichkorn *et al.*[69] The size of the TZQ+*g* basis set is (8s8p7d3f4g)/[4s4p4d3f2g] for Zr and (8s8p7d4f4g)/[4s4p4d3f2g] for Ag and Mo.

IV. Spin-orbit coupling

The DFT calculations do not include spin-orbit coupling, and to compare to experiment this must be included. For the general process AB → A + B we must consider three possible spin-orbit energies, namely those for AB, A, and B. Dissociation energies in this paper are computed by the formula

$$D_e = D_e(\mathrm{DFT}) + \Delta E_{SO} \qquad (1)$$

where

$$\Delta E_{SO} \equiv E_{SO}(\mathrm{A}) + E_{SO}(\mathrm{B}) - E_{SO}(\mathrm{AB}) \qquad (2)$$

where all values on the right-hand side are negative numbers because the spin-orbit effect lowers the energy of the ground state. Since our goal is to test DFT for the non-spin-orbit part of the energy, we used the most accurate available estimates for spin-orbit energy so that errors in the spin-orbit energy are negligible and do not affect our conclusions. Note that each value of D_e(DFT) in eq. (1) is calculated at the theoretical value of r_e for a given molecule and a given DFT method.

The spin-orbit effects for the atoms were calculated from the *J*-averaged spin-orbit levels for the atomic ground states from the atomic spectral information listed in Moore's reference books.[70] The spin-orbit effects for dimers were estimated using the first order approximation for the splitting of a multiplet term given by equation (V,8) in

Herzberg's book.[71] This only estimates the splitting of a multiplet term and does not account for the mixing of electronic states, which is also a spin-orbit effect.[72] For example, the Ni dimer is best described as a 0_g^+ state, which is a mix of the $^3\Pi_g$ and $^1\Pi_u^+$ states.[22] But, neither of the two states in Ni_2 will split since they are sigma states. The only dimer present in TMAE9/05 that has been experimentally shown to not have a Π ground state state is the Zr dimer, which is a $^3\Pi_g$ state.[24] We have estimated the spin-orbit splitting for Zr_2 using the approximate value of the spin-orbit coupling constant given by Doverstål *et al.,*[24] which yields an $E_{SO}(Zr_2) = -0.82$ kcal/mol. The final spin-orbit corrections are given in Table 3 and are denoted as ΔE_{SO}. Although the ground states calculated by DFT methods tend to not always agree with experiment or WFT, we nevertheless use the accurate spin-orbit energy in Eq. (2) so that tests presented here are always equivalent to comparing experimental dissociation energies that have the experimental spin-orbit effect removed to DFT calculations without spin-orbit effects.

V. Results and Discussion

V.A. Ground states. One of the characteristics that makes the theoretical study of transition elements challenging is the large number of low-lying electronic states. An extreme case is Ni_2 which has been shown to have nearly 60 states within 1 eV of the ground state.[73] To make matters even more complicated, DFT-based methods do not always predict the same ground states for the atoms and molecules as *ab initio* calculations or as is observed experimentally. In this paper, we do not force the dimers or atoms to have electronic configurations that agree with *ab initio* calculations or experimental results, but rather we always chose the atomic reference and dimer energies

to be the ones with the lowest energies for each method. In order to apply this choice consistently, we have calculated the energies for several different electronic states with all of the DFT methods for each dimer and atom and calculated the dissociation energy from the ground state predicted by each method. This is very labor intensive, but it ensures that we have indeed found the ground state predicted by each DFT method for each dimer and atom and that all tests of the theory are based on the ground-state binding energy predicted by each level of theory.

V.B. Atoms. The atomic ground states may be either $Ns^2(N-1)d^n$, $Ns^1(N-1)d^n$, or $Ns^1(N-1)d^{n+1}$ where N is the highest principal quantum number of the atom and n is the number of d-electrons in shell $N-1$. For the systems studied in this paper, experimental results show that Ag, Cr, Cu, and Mo have $Ns^1(N-1)d^n$ configurations and Ni, V, and Zr have are known to have $Ns^2(N-1)d^n$ configurations. But, it is known that DFT methods will favor the $Ns^1(N-1)d^{n+1}$ configuration over the $Ns^2(N-1)d^n$ configuration for systems such as Ni, V, or Zr. Yanagisawa *et al.*[14] has said that DFT will over stabilize the $Ns^1(N-1)d^{n+1}$ states relative to the $Ns^2(N-1)d^n$ states because the exchange functionals are not long-ranged enough, while Becke[74] suggested that the lack of current density in existing functionals destroys the degeneracy of partially occupied degenerate orbitals and raises the energy of some states relative to other states. Therefore, one will calculate a higher energy for states with a non-zero component of angular momentum ($M_L \neq 0$). However, it is not clear if these issues are the same since it is possible to have an $M_L = 0$ state with either an $Ns^2(N-1)d^n$ or $Ns^1(N-1)d^{n+1}$ configuration. Baerends *et al.*[75] has recommended that one use the average of configuration (AOC) method to calculate the reference, which involves computing the

energy from a density that is averaged over all of the electron configurations, whereas we always use the lowest-energy state.

Despite the unresolved issue of *why* DFT will over stabilize $Ns^1(N-1)d^{n+1}$ states, we have tested all of the methods to see *if* this is true for all methods or for specific types of methods, or if one gets qualitatively different results by using LSDA, GGA, hybrid GGA, meta GGA, and hybrid meta GGA. Since Ag, Cr, Cu, and Mo have $Ns^1(N-1)d^{n+1}$ ground states, and they are not expected to be a problem. We have checked the ground states of these atoms with all of the methods and both basis levels, and we found that all of the methods with both basis levels predicted the $Ns^1(N-1)d^{n+1}$ configuration with no mixing. For Ni, the $Ns^1(N-1)d^{n+1}$ and $Ns^2(N-1)d^n$ states have the same multiplicity (triplet), and thus one would expect a mixed state.

We calculated the atomic energies with several different guesses for each atom to assure ourselves that we had indeed found the lowest energy electronic configuration for each method, and we did a natural bond order analysis[76] to determine the electronic state of the atom. The results for Ni, V, and Zr are summarized in Table 4. Ni will be discussed first. It can be seen that the predicted ground states depend not only on the functional used, but also on the basis level. The GGA methods prefer a mixed state when the DZQ basis level is used, whereas 17% of the GGA methods predict no mixing when the TZQ basis level is used. Several of the hybrid GGA methods predict a mixed state when the DZQ level is used, and all hybrid GGA methods predict $4s^13d^9$ unmixed states when the TZQ basis level is used. Meta GGA methods tends to predict a mixed state with both basis levels. Interestingly, BB95 and mPWB95 both predict an unmixed $4s^23d^8$ with the DZQ level and an unmixed $4s^13d^9$ state with the TZQ level. The only

hybrid meta GGA method that predicts a mixed state is B1B95/DZQ. Both LSDA methods predict a mixed state with the DZQ basis level and an unmixed state with the TZQ basis level. It is interesting to note that HF predicts an unmixed $4s^2 3d^8$ state with both basis levels.

None of the DFT methods predict a mixed state for V or Zr. In general, the $4s^1 3d^4$ state is lower in energy than the experimental configuration of $4s^2 3d^3$ for V. With few exceptions (HCTH/DZQ and VSXC/DZQ), non-hybrid and hybrid meta methods predict a $4s^1 3d^4$ state, and the hybrid GGA predict both electronic configurations. In general, the DFT methods tested in this paper predict a $5s^2 4d^2$ state for Zr, which is the experimental ground state. No obvious trends are present in the Zr data since 57% of the methods predict a $5s^2 4d^2$ state with the DZQ and TZQ basis level level; however, different methods predict a $5s^2 4d^2$ ground state with the DZQ and TZQ basis levels. The only methods that predict the experimental ground states for Ni, V, and Zr are B97-1/DZQ, B98/DZQ, HF/DZQ, and HF/TZQ.

V.C. Ag_2, AgCu, Cu_2, V_2, Zr_2, and ZrV. All of the DFT methods (with the DZQ and TZQ basis levels) predict that Ag_2 and Cu_2 are both $^1\Sigma_g^+$ states and AgCu is a $^1\Pi$ state, which agrees with experimental results,[26] *ab initio* results,[77] and recent DFT results.[12] There is experimental evidence[78] and theoretical evidence[12,13] that V_2 has a $^3\Sigma_g^-$ ground state, which is in agreement with the ground states predicted by all of the DFT methods used in this paper. Recent experimental results indicate that the ground state of Zr_2 is $^3\Sigma_g$,[24] which is in disagreement with an earlier *ab initio* WFT studies that examined a large number of electronic states and predicted a singlet state.[79,80] A more

recent study showed that *ab initio* WFT methods predict a $^1\Sigma_g^+$ state, and DFT methods predict a $^3\Sigma_g$ state.[14] All of our calculations indicate that the ground state of Zr_2 is $^3\Sigma_g$. The ground state of ZrV has been determined experimentally to be a $^4\Phi$ state,[81] which is in agreement with all of our calculated results.

V.D. Ni_2. The ground state of Ni_2 has been somewhat controversial. Several DFT calculations indicate that the ground state is $^3\Sigma_g^-$,[17] hybrid DFT calculations with spin- and symmetry-projection methods predict that the ground state is a singlet,[82] *ab initio* WFT calculations indicate that the ground state is either a $^3\Sigma_g^-$ or $^3\Sigma_u^+$ state,[14] and earlier theoretical work predicts a singlet state.[83] The most plausible possibility is a Ω = 0 state of 0_g^+ symmetry (a mix of $^3\Sigma_g^-$ and $^1\Sigma_u^+$ state), but this is impossible to characterize unless spin-orbit coupling is included in the calculation.[22] We have calculated 11 different low-energy states for Ni_2. We note that our tests included multiple $^3\Sigma_g^-$ states, in particular the ($\sigma\sigma$) hole state suggested by Gustev and Bauschlicher,[17] and the ($\pi\pi$) hole state suggested by Yanagisawa *et al.*[13] We examined 5 singlet states and found all of these states to be slightly higher in energy than all of the triplet states. All of the singlets were computed as open-shell systems, but were not spin or symmetry adapted or projected. The ground states for the different methods are given in Table 5. Table 5 shows that the energetically competitive states are $^3\Pi_u$, $^3\Delta_u$, $^3\Phi_g$, and $^3\Sigma_u^+$. We did not find the $^3\Sigma_g^-$ state to have the lowest energy for any of the methods except the LSDA ones, both of which predict $^3\Sigma_g^-$ to be the ground state.

V.E. Cr_2 and Mo_2. The electronic structures of Cr_2 and Mo_2 are said to be antiferromagnetically aligned.[12,14,84-86] This means that the atoms in Cr_2 and Mo_2 will have $4s^1 3d^5$ electronic configurations where all of the electrons on one of the atoms are spin-up, and all of the electrons on the other atom will be spin-down. The quantitative description of these dimers using single-reference methods, such as DFT, can be improved by reducing the symmetry of the wave function from $D_{\infty h}$ to $C_{\infty v}$, which can be done by placing two He atoms along the internuclear axis at distances of –95 and 110 Å. We refer to this technique as a broken-symmetry calculation[87] (although others have sometimes used the term broken-symmetry to refer to any spin-unrestricted calculation). The broken-symmetry calculations will result in a spin-contaminated state. We also calculated the energies of several systems using $D_{\infty h}$ symmetry to ensure that the $C_{\infty v}$ energies are lower. We also tried other approaches, such as converging an antiferromagnetic singlet state and then using that wave function as the starting point for a triplet state. We also used several different guesses for the broken-symmetry calculations and found that the most reliable method was to first calculate the energy of CrMn (with two He atoms) and then use that wave function (with one less electron) as a starting point for both the Cr_2 and Mo_2 calculations. By starting with a CrMn wave function (minus one electron), we were able to reliably generate an antiferromagnetic set of guess orbitals for the Cr_2 and Mo_2 calculations.

The need for broken-symmetry calculations is tied to the unique bonding character of these dimers. An astute explanation of this was proposed by Baykara *et al.*,[87] who point out that for Cr_2, the π-MO orbitals of opposite spins are significantly localized and hence the spin densities have $C_{\infty v}$ symmetry and not $D_{\infty h}$ symmetry. If the

symmetry is not broken, one will form symmetry-adapted MOs and form a hextuple-bond configuration, which may be much more unstable. Baykara *et al*.[87] found that the molecular orbitals were not significantly localized for Mo_2 near the equilibrium distance. But, one will need to use broken symmetry to correctly describe the dissociation of the dimer.

Broken-symmetry calculations significantly reduce the energy for Cr_2 for all of the hybrid and non-hybrid methods. In fact, the chromium dimer is not even bound for all of the hybrid methods and several of the non-hybrid methods unless one does a broken-symmetry calculation. The situation is somewhat different for Mo_2. The $C_{\infty v}$ wave function either predicts the same energy as the $D_{\infty h}$ solution, whereas the hybrid methods predict lower energies when $C_{\infty v}$ symmetry is used. For the hybrid methods, the broken-symmetry calculations lower the energy of Mo_2 by an average of 19 kcal/mol.

It is interesting to examine the potential energy curves for both Cr_2 and Mo_2 since they have a very unique double-well structure that was first proposed by Goodgame and Goddard.[88] It has been argued that the potential curve for Cr_2 is more of a shelf than a double well, which was also observed experimentally for Cr_2 by Casey *et al.*;[29] and a recent high-level *ab initio* (CASPT2) study done by Roos[89] also confirms this shape. It was pointed out by Bauschlicher and Partridge[90] that non-hybrid GGA methods predict a qualitatively correct curve whereas hybrid GGA does not. However, recently Desmarais *et al*.[91] have showed that the PBE (GGA) functional predicts a slight double-well potential for Cr_2, although the global shape of the potential looks incorrect. A recent

multireference study of Mo_2 by Balasubramanian and Zhu[92] also does not predict a double well potential.

We have computed the potential energy curve with 5 different DFT methods (BLYP, mPWKCIS, MPW1B95, MPW1KCIS, and PBE) with the TZQ basis level. The hybrid methods that we used were chosen in part because they differ significantly in the amount of HF exchange, in particular the MPW1KCIS and MPW1B95 methods use 15 and 31 percent HF exchange, respectively. The non-hybrid methods were chosen because they represent a diverse set of methods: BLYP is a first-generation GGA method, whereas PBE is considered a second-generation GGA functional, and mPWKCIS is fundamentally different from either of those methods because it is a meta GGA method. The potential energy curves for Cr_2 and Mo_2 are shown in Figs. 1 and 2, respectively.

Fig. 1 shows that there are significant qualitative and quantitative differences between the hybrid and non-hybrid methods for Cr_2. The hybrid GGA methods do not predict the inner well that is predicted by the GGA, meta GGA, and high-level *ab initio* WFT methods and that is seen experimentally. This was pointed out earlier by Bauschlicher and Partridge,[90] but they did not study hybrid meta GGA methods, and it appears that incorporating the kinetic energy density into the functionals does not change this aspect of hybrid methods. We will return to this shortly. The non-hybrid methods all predict the shelf for Cr_2, but the shelf is least distinct for BLYP. Also, our PBE curve for Cr_2 looks somewhat different from the PBE curve calculated by Desmarais *et al*.[91] Specifically, our curve differs qualitatively because it predicts a shelf and not the double-well, and the overall shape of our curve tends to agree better with the experimental and

ab initio curves of Casey and Leopold[29] and Roos,[89] respectively, than does the PBE curve of Desmarais *et al*.[91]

Fig. 2 shows that there are fewer qualitative differences between the hybrid and non-hybrid methods for the potential energy curve of Mo_2. None of the methods that we tested predicts a double well potential for Mo_2, and our results tend to agree better with the WFT results of Balasubramanian and Zhu[92] than the earlier results of Goodgame and Goddard.[88] The most striking difference between the hybrid and non-hybrid methods is the well depths. All of the methods underestimate the binding energy, but the non-hybrid methods agree with experiment better than the hybrid methods. BLYP, mPWKCIS, and PBE underestimate the binding energy by 1, 16, and 17 kcal/mol, respectively, and the MPW1B95 and MPW1KCIS functionals underestimate the binding energy by 69 and 45 kcal/mol, respectively.

Returning once again to the potential energy curve for Cr_2, the results by Bauschlicher and Partridge[90] and the results presented here (the MPW1B95 and MPW1KCIS potential energy curves) indicate that perhaps any amount of Hartree–Fock exchange would cause the inner-well to disappear. We tested the sensitivity of the potential energy curve for Cr_2 to the amount of Hartree–Fock exchange by using the mPW exchange functional and the KCIS correlation functional (mPWKCIS) and varying the fraction of Hartree–Fock exchange from 0% to 8% with 1% increments. Fig. 3 shows that the curve is very sensitive to the amount of Hartree–Fock exchange. In particular, the inner well rapidly disappears when the fraction of Hartree–Fock exchange is increased from 0%. Interestingly, the addition of exact exchange leads to a double-well potential when $X = 3\%$. The inner-well is effectively gone by the time the fraction

of Hartree–Fock exchange is 8%, and an ancillary effect of this is a significant overestimation of the bond length for hybrid methods. Fig. 4 is a histogram of the bond lengths computed with the various methods using the TZQ basis level and shows that all of the hybrid methods significantly overestimate the bond length (1.68 Å). The non-hybrid methods, with a few exceptions, agree well with the experimental bond length for Cr_2. The exceptions are HCTH, OLYP, SPWL, and VSXC, which predict the bond lengths to be 2.46, 2.54, 2.38, and 2.25 Å, respectively.

V.F. Atomization energies. The errors for the atomization energies are given in Table 6. The table gives mean signed error (MSE), mean unsigned error (MUE), and root-mean-squared error (RMSE), as well as the average of MUE (AMUE) with the two basis sets. The error is taken as the difference between theory and experiment, so a negative MSE indicates that the methods under bind and a positive MSE indicates that the methods over bind. The AMUE denotes the average mean unsigned error and is the average of the MUEs with the DZQ and TZQ basis levels. The AMUE is included because it is favorable to have a DFT method that works well with both large and small basis sets. For example, we would like our conclusions to be valid at the small molecule limit as well as the nanoparticle regime where system sizes preclude the use of large basis sets. One will see that certain DFT methods, like B97-2, have small errors with the TZQ basis set, but much larger errors with the DZQ basis set which is perhaps because the methods were parameterized with specific basis sets.

On average, the non-hybrid methods are far superior to the hybrid methods. The AMUEs for the GGA and meta GGA methods are 7.0 and 8.8 kcal/mol, respectively. These errors are significantly lower than the errors for hybrid GGA and hybrid meta

GGA, which are 20.9 kcal/mol and 21.8 kcal/mol, respectively. The hybrid methods yield an improvement over the LSDA results, which have an AMUE of 26.8 kcal/mol. The best GGA, hybrid GGA, meta GGA, and hybrid meta GGA methods are BLYP, B97-2, mPWKCIS, and TPSSh, respectively. BLYP is the best method and has an AMUE of 4.3 kcal/mol. Several other GGA methods have errors that are comparable to BLYP, notably XLYP and G96LYP, which have errors of 5.1 and 5.6 kcal/mol, respectively. B97-2 and TPSSh have AMUEs of 9.4 and 13.2 kcal/mol, respectively. The best meta GGA method (mPWKCIS) has an AMUE of 6.3 kcal/mol.

Fig. 5 plots the signed errors in atomization energies for the dimers in TMAE9/05 for BLYP/DZQ, BLYP/TZQ, and BLYP/TZQ+*g*. The signed errors are only plotted for BLYP, but most of the DFT methods show similar trends. It can be seen that BLYP/DZQ underestimates the atomization energy for Mo_2 by 15 kcal/mol, whereas BLYP/TZQ underestimates the atomization energy for Mo_2 by less than a 1 kcal/mol. Therefore, one could conclude that *f*-polarization functions are very important in accurately calculating the atomization energy of Mo_2, but one will also notice that the magnitude of the signed errors become noticeably larger for the atomization energies of Ni_2 and V_2 when the TZQ basis set is used in place of the DZQ basis set. One could speculate that *g*-functions may be necessary for proper treatment of the 4*d* transition metals if they significantly increase the binding energy of the 4*d* dimers, in which case the 4*d* dimers would have signed errors that are consistent with those of the 3*d* dimers. We have tested this hypothesis using the TZQ+*g* basis set with the BLYP method. The magnitudes of the signed errors for the dimers computed with the BLYP/TZQ+*g* (Fig. 5) method are not significantly larger than the signed errors with BLYP/TZQ. The addition

of *g*-functions only increases the binding energies, with respect to the TZQ basis set for Ag_2, CuAg, Mo_2, Zr_2, and ZrV by 1.2, 1.5, 2.1, 0.1, and 1.7 kcal/mol, respectively. This is not a very thorough study of the effects of adding *g*-polarization functions to the basis set, but it does gives us some level of confidence that the TZQ basis set is large enough to draw reasonable conclusions about the accuracy of the DFT methods tested in this paper.

The addition of polarization functions (both *f* and *g*) has a much smaller effect on the bond energies of the coinage metals (Cu_2, CuAg, and Ag_2) than the other dimers in TMAE9/05, which is in agreement with previous studies.[93] This trend is consistent with the bond being $4s\sigma_g$ in character.[26] Neverthelss, *d* orbitals are important for an accurate description of the bonding, as has been shown with correlated WFT calculations of the coinage dimers.[11,94]

To put the results in this paper in a broad perspective, we have computed the MUE for all of the DFT methods in this paper against two other previously published databases,[95] AE6 (6 atomization energies of molecules, especially organic chemicals, that are composed of main group elements) and BH6 (six barrier heights), and Table 7 compares these results with the MUEs for the transition metal dimers computed with the TZQ basis set. It is seen that not one method that does well for main group chemistry and barrier heights does well for transition metals. In fact, the methods that are that best at predicting barrier heights are among the absolute worst methods for transition metals. Likewise, the most accurate methods for transition metals are among some of the worst methods for main group atomization energies and barrier heights. Even within a category of DFT methods and with similar values of *X*, this reverse trend is clear; compare, for example, the results for B3P86 to either mPW1PW91 or PBE1PBE. However, the B97-2

method is truly unique, in that, although it is not "the best" method for any of the tests considered here, it does remarkably well when tested against AE6 and TMAE9/05 and has "reasonable" MUEs for barrier heights. The MUE in barrier heights is 3.21 kcal/mol, and this is roughly 1 kcal/mol less than the MUEs for most of the hybrid methods (those with $X < 28\%$) and about a 5 kcal/mol smaller MUE than the MUEs for the non-hybrid methods.

Becke has pointed out that atomic and molecular systems with $M_L = 0$ have a lower DFT energy than systems with nonzero M_L (although, of course, they should be degenerate) and that the inclusion of current density is necessary to fix this and will be critical to the success of any DFT method.[74] We have made a subset of the data that contains only atoms and molecules that can only have zero current density. This subset consists of Ag_2, Cr_2, CuAg, Cu_2, and Mo_2. This subset was chosen because neither the atoms nor molecules have current density. The errors in atomization energy for Ag_2, CuAg, Cu_2, Cr_2, and Mo_2 are presented in Table 8. The errors are slightly lower (on average) for this subset of the data, but our conclusions remain the same. The non-hyrbid DFT methods are more accurate than the hybrid DFT methods, and BLYP still has the smallest AMUE. The AMUE of BLYP when tested against the entire data set is 4.3 kcal/mol and is 3.5 kcal/mol when tested against Ag_2, CuAg, Cu_2, Cr_2, and Mo_2. The signed errors for BLYP/DZQ, BLYP/TZQ, and BLYP/TZQ+*g* are plotted in Fig. 5 and one can see that the errors in this subset for BLYP are due primarily to an underestimation of the bond energy for Mo_2 when the DZQ basis level is used and an overestimation of the bond energy for Cr_2 when the TZQ basis level is used. For BLYP, the errors are small for Ag_2, CuAg, Cu_2 with the DZQ and TZQ basis levels; however,

Cr_2 has a small error with the DZQ basis set and a much larger error with the TZQ basis set, whereas Mo_2 has a large error with the DZQ basis set and a small error with the TZQ basis set. Many of the other methods, specifically the hybrid methods, have large errors with both basis sets for Cr_2 and Mo_2. It can be argued that Ag_2, CuAg, Cu_2 are significantly different than Cr_2 and Mo_2 since Ag_2, CuAg, Cu_2 have no direct contribution from the *d*-orbitals to the chemical bonding, and the dissociation limit (Cu and Ag) has a closed *d*-subshell. As a consequence, the coinage dimers do not have a manifold of nearly degenerate electronic states. At a minimum, the first excited electronic state for any coinage dimer is 11,000 cm^{-1} (31 kcal/mol) above the ground state.[26]

A key issue that may explain the trends in the previous paragraph is that the coinage dimers can be quantitatively described using single-reference methods such as MP2 or CCSD(T), whereas Cr_2 and Mo_2 cannot be described using such methods.[13,14,77,90] Specifically, Yanagisawa *et al.*[13,14] have shown that Cr_2 and Mo_2 are unbound using MP2, and Bauschlicher and Partridge[90] have shown that Cr_2 is unbound using restricted CCSD(T) and significantly underbound using unrestricted CCSD(T).[90] These results indicate Cr_2 and Mo_2 have significant multi-reference character and cannot be treated using single-reference methods. The amount of multireference character present can be understood by examining the weights of the Hartree–Fock configuration in the multiconfiguration wave function. For the Cr_2 this weight is 45%,[89] and the weight is 68% for Mo_2.[92] These studies were done by different groups and used different computational methods, so the comparison of weights is semiquantitative. Although there have been numerous *ab initio* multiconfigurational studies of the coinage dimers,

we are unaware of any published weights for the Hartree–Fock configurations in these molecules.

In light of the above considerations, we consider another subset of the data that contains only the atomization energies of systems that do not have significant amounts of multireference character. It is difficult to establish a prescription for selecting which pieces of data should be included in the subset. The published tables by Yanagisawa *et al.*[13,14] reveals that about half of the dimers are bound by MP2 and about half are unbound. Using this as a guide, we have made a subset of the data in which the dimers have positive MP2 binding energies. The dimers that are included are Ag_2, CuAg, Cu_2, and Zr_2. The $^3\Sigma_u^+$ of Ni_2 is bound, but the $^3\Sigma_g^-$ state has a negative binding energy, and the high-level *ab initio* calculations by Yanagisawa *et al.*[13,14] predict a separation of only 0.02 eV. This leads us to believe that the MP2 results are unphysical. The two lowest-energy structures of the Zr dimer are bound, but have large errors in the atomization energies. The most recent *ab initio* multireference study of Zr_2 indicates that the weights for the Hartree–Fock configuration of the ground and first few excited states are between 85% and 87%,[80] which is larger than either Cr_2 or Mo_2 and leads us to include Zr_2 in the "single reference" subset.

The errors in atomization energies for Ag_2, CuAg, Cu_2, and Zr_2 are given in Table 9, which will be discussed in this paragraph. The average MUEs for the GGA and hybrid GGA methods against the "single reference" subset are 3.2 kcal/mol and 7.1 kcal/mol, respectively. There is also significant improvement for the meta methods when they are tested only against the "single refence" subset, the average MUEs of all of the meta GGA and hybrid meta GGA methods are 5.1 and 6.2 kcal/mol, respectively. These

errors are significantly larger than the errors in Table 6. BPBE, BPW91, and TPSSh all have AMUEs of 1.5 kcal/mol for this subset of data (Ag_2, CuAg, Cu_2, and Zr_2); however, preference is given to TPSSh since the MUE decreases when one goes from the DZQ basis level to the TZQ basis level, whereas the MUE increases for BPBE and BPW91 when one goes from the DZQ basis level to the TZQ basis level; thus the TPSSh method has the lowest error (1.3 kcal/mol) when only the TZQ basis level is considered. It is interesting to note that the errors at the TPSSh/TZQ level are systematic in that the mean signed and unsigned errors are –1.3 and 1.3 kcal/mol respectively, and the mean signed and unsigned errors for TPSS/TZQ (the non-hybrid counterpart of TPSSh/TZQ) are both 2.4 kcal/mol, which indicates that 10% HF exchange is still too much. The accuracy of BLYP for this subset is still comparable to that of TPSSh. The AMUE for BLYP is only 0.2 kcal/mol higher than TPSSh, and the errors also decrease when the basis set is increased. The MUEs for BLYP/DZQ and BLYP/TZQ are 1.9 and 1.5 kcal/mol. The critical issue is not that TPSSh/TZQ has a MUE that is 0.2 kcal/mol lower than BLYP/TZQ, but that we have shown that mixing in single-reference exchange (HF exchange energy) with DFT exchange results in large errors when tested against the entire database, whereas mixing in HF exchange is not as deleterious for dimers that have smaller amounts of multireference character. Another related issue that may be considered is spin contamination, which we discuss in the Supporting Information.

Although we attempt to base the comparisons in this paper on particular reliable experimental data, some of the experimental errors (for example, that for AgCu) are comparable to the smaller mean errors in Table 9. If one were to calculate the errors in the DFT methods as deviation from the edge of the experimental range rather that its

center, the DFT errors would be even lower. We did not include this refinement in our calculations of mean errors.

V.G. Representative database. When designing the databases, we tried to keep their sizes manageable to facilitate studying a large number of methods. However, we found that even studying 9 transition metal dimers is a formidable task due to the manifold of nearly degenerate electronic states that must be examined and the numerous SCF convergence issues for both the atoms and the dimers. Making the database even smaller would alleviate some of the difficulty in testing and developing new DFT methods. Previous work by Lynch and Truhlar[95] has shown that small representative subsets can nearly reproduce the errors of much larger data sets.

Following the prescription by Lynch and Truhlar,[95] we find a subset that minimizes the root-mean-square-deviation (RMSD) between the three standard errors (MSE, MUE, and RMSE) calculated using TMAE9/05 and same errors using a small subset, e.g., the deviation between the MSE using TMAE9/05 (*MSE*(*TMAE9*)) and the MSE using a small subset (*MSE*(*SS*)). The RMSD is calculated using eq 1, where we sum the errors of all 84

methods (42 DFT methods with two basis levels)

$$RMSD = \left\{ \frac{1}{252} \sum_{i=1}^{84} \left[\left(MSE_i(TMAE9) - MSE_i(SS) \right) \right]^2 \right. \\ \left. + \left[\left(MUE_i(TMAE93) - MUE_i(SS) \right) \right]^2 + \left[\left(RMSE_i(TMAE9) - RMSE_i(SS) \right) \right]^2 \right\}^{\frac{1}{2}} \quad (3)$$

The mean error (ME) is defined as

$$\mathrm{ME} = \left\{ \frac{1}{252} \sum_{i=1}^{84} \left(\left| MSE_i(TMAE9) \right| + MUE_i(TMAE9) + RMSE_i(TMAE9) \right) \right. \quad (4)$$

and finally the percentage error in representation is defined as

$$\mathrm{PEIR} = 100\% \times \frac{\mathrm{RMSD}}{\mathrm{ME}}. \qquad (5)$$

We have examined all possible subsets with *n* dimers (*n* = 2 – 8) and found the lowest RMSD for each possible subset of *n* dimers. The PEIRs for each set of subset of dimers with *n* = 2 – 8 are 27, 21, 14, 10, 10, 7, and 6%, respectively.

The best compromise between low PEIR on the one hand and low cost and good diversity of the other is for *n* = 4. This subset of data contains Cr_2, Cu_2, V_2, and Zr_2, and we will call the subset of data set TMAE4/05. (It might at first seem surprising that the subset of data for *n* = 5 is the complement of the *n* = 4 set and contains the atomization energies of Ag_2, CuAg, Mo_2, Ni_2, and ZrV; however, it is not really surprising since if a subset is represenative, then so must be its complement, at least numerically.) The subset of 4 dimers represents a significant reduction in computational effort because over 50% of the molecules are removed, and the most problematic case (Ni_2) is removed. Ni_2 is not called problematic because the DFT methods have large errors, but rather because the large number of nearly degenerate states forces one to examine a large number of electronic states, which is extremely time consuming. Also, assuring ourselves that we had found the lowest energy solution for the Ni atom was also very challenging and required numerous calculations for every functional.

The errors in atomization energy for Cu_2, Cr_2, V_2, and Zr_2 are given in Table 10. As shown in Table 14, similar conclusions would be drawn by only considering the AMUEs for each method. In particular, the BLYP is still the best method (AMUE of 4.5 kcal/mol against TMAE4/05 and 4.3 kcal/mol against TMAE9/05). The average unsigned difference between the AMUEs computed with TMAE4/05 and TMAE9/05 is

1.1 kcal/mol. However, there are some inconsistencies among other errors. Again, using BLYP as an example, compare the MUEs with the DZQ and TZQ basis sets. So, in a sense, the TMAE4/05 database is the most representative set of data in a numerical sense, but it is not a perfect representation of the TMAE9/05 database. Nevertheless, we recommend it for further testing and even for development work, when time does not permit the use of the TMAE9/05 database.

V.H. Bond lengths. The errors for bond lengths are given in Table 11, and these results show that the non-hybrid methods are again more accurate than the hybrid methods. The meta DFT methods are slightly less accurate than the non-meta DFT methods. The average AMUEs for the GGA and meta GGA methods are 0.09 and 0.11 Å, respectively. The average AMUEs for the hybrid GGA and hybrid meta GGA methods are 0.19 and 0.17 Å, respectively. The LSDA methods are markedly better than the hybrid methods for bond lengths, which have an AMUE of 0.05 Å. The best methods overall are SVWN3 and SPWL (both LSDA), which have AMUEs of 0.05 Å. The errors are also very sensitive to the basis level, especially for the non-hybrid methods. The AMUE for the GGA methods with the DZQ and TZQ basis levels are 0.13 and 0.05 Å, respectively, and the AMUE for the meta GGA methods with the DZQ and TZQ basis levels are 0.14 and 0.08 Å, respectively. The hybrid methods are much less sensitive to the addition of polarization functions. The AMUEs for the hybrid GGA methods with the DZQ and TZQ basis levels are both 0.19 Å. The AMUEs for the hybrid meta GGA methods with DZQ and TZQ basis levels are 0.16 and 0.14 Å, respectively.

The fact that the GGA is not always superior to the LSDA is well known from previous work, as reviewed elsewhere,[6] but the present article shows that for bond

lengths in transition metal dimers, this extends even to the latest and most advanced GGAs. It is hard to escape the conclusion, though, that the good performance of SVWN3 and SPWL in Table 11 results, at least in part, from a cancellation of errors, given the large energetic errors of these two methods in Table 6. Nevertheless, any method that performs best on average out of 42 serious candidates for a carefully selected set of diverse cases deserves further consideration. We have also included the HF bond lengths in Table 11. It can be seen that the hybrid methods have MUEs that are between the errors of HF and the GGA methods.

One important aspect of careful checking of theory against experiment is to double check the lore of the field and ascertain if (or under what conditions) general impressions of the field are actually true. For example, a key review of DFT[1] states that LSDA yields bond lengths of molecules accurate to 1%; that would be ~0.02 Å. Table 11 shows that none of the 42 density functionals considered here achieve that accuracy or anything close to it.

As mentioned earlier, several of the DFT methods cannot predict a qualitatively correct potential energy curve for Cr_2, and we attribute this to the multireference character of Cr_2. In Table 12, we present the errors for the bond lengths for our single-reference subset (Ag_2, AgCu, Cu_2, and Zr_2); this more restricted test significantly changes the landscape for the hybrid methods in respects to bond lengths as it also did for bond energies. The hybrid methods are no longer significantly worse than the non-hybrid methods, and, in fact, the hybrid meta GGA methods are among the most accurate methods with an average MUE of 0.04 Å. The average MUE of the GGA, hybrid GGA, and meta GGA methods are 0.05, 0.05, and 0.05 Å, respectively. The methods with the

lowest AMUEs are SPWL, B3P86, and TPSS1KCIS which have AMUES of 0.03 Å. It is very interesting to point out that if we exclude LSDA methods, the remaining 160 mean signed errors in Table 11 and 12 are all positive or 0.00 Å. For this subset, we note that the MUEs in the HF bond lengths decrease by almost 50%, but the hybrid methods are no longer intermediate between the HF and GGA results.

The errors are also less sensitive to the basis set for the single-reference subset. For the hybrid meta DFT methods, the average MUE with the DZQ and TZQ basis levels are both 0.04 Å. Similar trends are observed for the other methods, where the additional of polarization and diffuse functions reduces the MUE by 0.00 – 0.02 Å. If we focus only on the TZQ basis level, the most accurate methods is TPSS1KCIS which has an MUE of 0.02 Å and numerous methods have errors of 0.03 Å.

V.I. Jacob's ladder. Perdew and coworkers[53,96,97] have created a sequence of parameter-free methods, namely SPWL, PBE, and TPSS, that are called the first three rungs of Jacob's ladder because they introduce new features successively. In particular, rung 2 (PBE) introduces gradient corrections, and rung 3 (TPSS) introduces kinetic energy density. The hope would be that performance improves as one climbs the ladder (although in the original story,[98] angels were passing up *and down* the ladder). Table 6 shows that bond energies improve going from the first rung to the second, but not in going to the third. Table 8 shows that this behavior is not corrected if we delete systems with current density; however, Table 10 shows that the desired trend is obtained if we delete systems with multireference character. Table 11 shows that TPSS does not improve over PBE for bond lengths, and Table 12 shows that this remains true even if we focus only on the single-reference dimers.

It is interesting to compare the conclusions here for bond lengths of transition metal dimers, with the conclusions of Perdew and coworkers[97] for lattice constants of bulk metals. In comparing the results we should keep in mind that lattice constants are larger than bond distances or nearest neighbor distances; in particular the average metal equilibrium lattice constant in their study is 4.03 Å, while the average equilibrium bond length in the present study is 2.10 Å (a factor of 1.9 smaller). Perdew and coworkers considered four main group bulk metals (Li, Na, K, and Al) and four transition metals (Cu, Rh, Pd, and Ag). Their errors are compared to ours in Table 13. Since Ref. 97 used a mixture of double zeta and triple zeta basis sets, the present results are averaged over the DZQ and TZQ basis sets. Since Cr_2 seems to be untypical, we discuss the comparison in terms of the results from Table 12, where Cr_2 is excluded. We also exclude the LSDA results for main group metals, since the LSDA is inaccurate in that case. The other bulk errors are comparable to the errors in Table 11, indicating that the percentage errors are typically smaller for the bulk than for the dimers. The PBE and TPSS lattice constants are too large in 15 out of 16 cases, a systematic error similar to the one we found for dimers. The SPWL and TPSS lattice constants are more accurate for transition metals than for main group metals, whereas PBE is more accurate for the main group. For main group lattice constants and transition element dimers, PBE is more accurate than TPSS, whereas for transition metal lattice constants, TPSS is more accurate than PBE. (However, Fuchs *et al.*[99] found several cases where DFT underestimates lattice constants for the main group bulk metals). All mean errors in Table 13 are larger than those anticipated in the 1998 review,[1] as discussed above.

VI. Conclusions

The main result of the present paper is the creation of diverse sets of carefully selected data for energies and equilibrium distances of bonds between transition elements, and their use for careful tests of the accuracy of DFT predictions of ground-state properties of systems with metal–metal bonds. In particular, we have presented three new databases in this paper: the TMAE9/05 and TMAE4/05 databases of atomization energies for transition element dimers and the TMBL8/05 database of bond lengths for transition element dimers. We have used these databases to study 42 different DFT methods.

The first key results of this paper are in the last column of Table 6, which contains an average over eighteen errors in predicted bond energies for each DFT method. Amazingly, although 39 of the 41 other density functionals are more recent than the seventeen-year-old BLYP (BP86 is the same age, and SVWN3 is older), none does better for dissociation energies of bonds between transition metals. The second best method is the recent (less than one year old) XLYP method. The second key result of this paper is the last column of Table 11, which is an average over fourteen errors in bond lengths for each DFT method. Here the absolutely oldest of the 42 functionals, the twenty-five-year-old SVWN3 functional, and the other LSDA functional, SPWL, does the best. Close behind is mPWLYP, which is followed by BLYP, BP86, G96LYP, and XLYP. In general, our results show that non-hybrid methods are far better than the hybrid methods for all three databases. Despite the tremendous amount of work that has been done in the area of developing new DFT methods, we recommend the older, well-established BLYP

method for atomization energies and geometries of transition element dimers and, by extension, transition element clusters, and nanoparticles.

In addition to identifying the best methods, our assessment illustrates other key trends in the reliability of various density functionals. For example, mixing Hartree–Fock exchange with explicit functionals of the density and density gradient, a procedure whose success is mainly responsible for the enormous popularity of density functional theory for applications in organic chemistry and other main group chemistry, is a disaster for the problems considered here. By considering various subsets of the data, we were able to show that the problem is severe when the system exhibits significant amounts of so called multireference character, also called static correlation or nondynamical correlation, a problem analyzed in informative detail by Tschinke and Ziegler[7]and Boijse and Baerends.[10] Systems with this characteristic have quite different one-electron densities in the Hartree-Fock and DFT approximations, with the latter being more accurate. For such systems, replacing any fraction of DFT exchange by HF exchange apparently makes the electron density less accurate, and even good functionals applied to inaccurate densities cannot yield reliable energetics or bond lengths.

Ultimately a useful choice of functionals must yield accurate results even with the presence of multireference character. Nevertheless, by focusing on cases without significant multireference character, we can test the ability of all the various functionals to make accurate energetic predictions from qualitatively correct electron densities. One could argue that the subset of data without multireference character should show trends similar to those found for organic chemistry, but this is not found to be the case. Further analysis of the results showed that if we eliminate dimers with significant multireference

character, the hybrid meta GGA method TPSSh performs slightly better than BLYP, but BLYP still has a very low error when examined over this subset, as shown in Table 9. Among methods that do well for organic chemistry (as determined in previous papers) the B97-2 functional is remarkable in also performing well for the main group data in Table 9. But none of the methods (MPW1K or BB1K) that does well for barrier heights, does well for transition element bonding.

The present article does not attempt a complete explanation of all the trends in the data. In that respect, it is only a first step. We hope that this first step will be useful for four purposes: (i) to provide useful feedback to functional development efforts of how various functionals developed so far actually perform; (ii) to enable those making applications of DFT to systems with metal–metal bonds to have realistic expectations about the accuracy that they can expect; (iii) to enable such practitioners to choose the most appropriate functionals for cases where numerical accuracy of the predictions is important and avoid functionals with demonstrated large errors; (iv) to spur developers to new efforts to try to improve on the somewhat disappointing accuracy of several of the classes of functionals.

The present findings present a significant challenge for DFT. The methods that work best for transition metals are quite different from those like mPW1PW91, MPW1B95, and MPW1K that work best for main group chemistry. The development of a universally accurate density functional remains an unmet goal.

VII. Acknowledgments

The authors are grateful to Doreen Leopold for helpful suggestions. This work is supported in part by the Defense-University Research Initiative in Nanotechnology

(DURINT) of the U. S. Army Research Laboratory and the U. S. Army Research Office under agreement number DAAD190110503 and also in part by the U.S. Deprt. of Energy, Office of Basis Energy Sciences. Computational resources were provided by the Minnesota Supercomputing Institute.

VIII. Supporting Information

The computed atomization energies and bond lengths for several DFT methods are given in Tables S4 – S6. We have also included a brief discussion about spin contamination, which is illustrated by Tables S1 – S3. This material is available free of charge via the Internet at http://pubs.acs.org.

IX. References

(1) Kohn, W. *Rev. Mod. Phys.* **1998**, *71*, 1253.
(2) Raghavachari, K.; Anderson, J. B. *J. Phys. Chem.* **1996**, *100*, 12960.
(3) Becke, A. D. *J. Chem. Phys.* **1993**, *98*, 5648.
(4) Baker, J.; Muir, M.; Andzelm, J.; Scheiner, A. *ACS Symp. Ser.* **1996**, *629*, 342.
(5) Zhao, Y.; Pu, J.; Lynch, B. J.; Truhlar, D. G. *Phys. Chem. Chem. Phys.* **2004**, *6*, 673.
(6) Perdew, J. P. Density Functional Theory of Molecules, Clusters, and Solids; Ellis, D. E., Ed.; Kluwer: Dordecht, 1995; pp 47-66.
(7) Tschinke, V.; Ziegler, T. A. *J. Chem. Phys.* **1990**, *93*, 8051.
(8) Gritsenko, O. V.; Schipper, P. R. T.; Baerends, E. J. *J. Chem. Phys.* **1997**, *107*, 5007.
(9) Handy, N. C.; Cohen, A. J. *Mol. Phys.* **2001**, *99*, 403.
(10) Buijse, M. A.; Baerends, E. J. Density Functional Theory of Molecules, Clusters, and Solids; Ellis, D. E., Ed.; Kluwer: Dordecht, 1995; pp 1-46.
(11) Langhoff, S. R.; Bauschlicher, C. W. J. *Annu. Rev. Phys. Chem.* **1988**, *39*, 181.
(12) Barden, C. J.; Rienstra-Kiracofe, J. C.; Schaefer, H. F. I. *J. Chem. Phys.* **2000**, *113*, 690.
(13) Yanagisawa, S.; Tsuneda, T.; Hirao, K. *J. Chem. Phys.* **2000**, *112*, 545.
(14) Yanagisawa, S.; Tsuneda, T.; Hirao, K. *J. Comput. Chem.* **2001**, *22*, 1995.
(15) Baker, J.; Pulay, P. *J. Comput. Chem.* **2003**, *24*, 1184.
(16) Wu, Z. J. *Chem. Phys. Lett.* **2004**, *383*, 251.
(17) Gustev, G. L.; Bauschlicher, C. W. J. *J. Phys. Chem. A* **2003**, *107*, 4755.

(18) Becke, A. D. *Phys. Rev. A* **1988**, *38*, 3098.

(19) Perdew, J. P. In *Electronic Structure of Solids '91*; Ziesche, P., Esching, H., Eds.; Akademie Verlag: Berlin, 1991.

(20) Lombardi, J. R.; Davis, B. *Chem. Rev.* **2002**, *102*, 2431.

(21) Morse, M. D. *Chem. Rev.* **1986**, *86*, 1049.

(22) Pinegar, J. C.; Langenberg, J. D.; Arrington, C. A.; Spain, E. M. *J. Chem. Phys.* **1995**, *102*, 666.

(23) Morse, M. D.; Hansen, G. P.; Langridge-Smith, P. R. R.; Zheng, L.-S.; Geusic, M. E.; Michalopoulos, D. L.; Smalley, R. E. *J. Chem. Phys.* **1984**, *80*, 5400.

(24) Doverstål, M.; Karlsson, L.; Lindgren, B.; Sassenberg, U. *J. Phys. B: At. Mol. Opt. Phys.* **1998**, *31*, 795.

(25) Bernath, P. F. *Spectra of Atoms and Molecules*; Oxford University Press: New York, 1995.

(26) Morse, M. D. *Chemical Bonding In The Late Transition Metals: The Nickel and Copper Group Dimers*; JAI Press Inc.: Greenwich, Conn., 1993; Vol. 1.

(27) Bishea, G. A.; Marak, N.; Morse, M. D. *J. Chem. Phys.* **1991**, *95*, 5618.

(28) Langenberg, J. D.; Morse, M. D. *Chem. Phys. Lett.* **1995**, *239*, 25.

(29) Casey, S. M.; Leopold, D. G. *J. Phys. Chem.* **1993**, *97*, 816.

(30) Fast, P. L.; Sanchez, M. L.; Corchado, J.; Truhlar, D. G. *J. Chem. Phys.* **1999**, *110*, 11679.

(31) Martin, J. M. L. *J. Chem. Phys.* **1992**, *97*, 5012.

(32) Frisch, M. J.; Trucks, G. W.; Schlegel, H. B.; Scuseria, G. E.; Robb, M. A.; Cheeseman, J. R.; J. A. Montgomery, J.; Vreven, T.; Kudin, K. N.; Burant, J. C.; Millam, J. M.; Iyengar, S. S.; Tomasi, J.; Barone, V.; Mennucci, B.; Cossi, M.; Scalmani, G.; Rega, N.; Petersson, G. A.; Nakatsuji, H.; Hada, M.; Ehara, M.; Toyota, K.; Fukuda, R.; Hasegawa, J.; Ishida, M.; Nakajima, T.; Honda, Y.; Kitao, O.; Nakai, H.; Klene, M.; Li, X.; Knox, J. E.; Hratchian, H. P.; Cross, J. B.; Adamo, C.; Jaramillo, J.; Gomperts, R.; Stratmann, R. E.; Yazyev, O.; Austin, A. J.; Cammi, R.; Pomelli, C.; Ochterski, J. W.; Ayala, P. Y.; Morokuma, K.; Voth, G. A.; Salvador, P.; Dannenberg, J. J.; Zakrzewski, V. G.; Dapprich, S.; Daniels, A. D.; Strain, M. C.; Farkas, O.; Malick, D. K.; Rabuck, A. D.; Raghavachari, K.; Foresman, J. B.; Ortiz, J. V.; Cui, Q.; Baboul, A. G.; S. Clifford; Cioslowski, J.; Stefanov, B. B.; Liu, G.; Liashenko, A.; P. Piskorz; Komaromi, I.; Martin, R. L.; Fox, D. J.; Keith, T.; M. A. Al-Laham; Peng, C. Y.; Nanayakkara, A.; Challacombe, M.; P. M. W. Gill; Johnson, B.; Chen, W.; Wong, M. W.; Gonzalez, C.; Pople, J. A. *Gaussian03*; Gaussian, Inc.: Pittsburgh, PA, 2003.

(33) Slater, J. C. *Quantum Theory of Molecules and Solids*; McGraw-Hill: New York, 1974; Vol. 4.

(34) Vosko, S. H.; Wilk, L.; Nusair, M. *Can. J. Phys.* **1980**, *58*, 1200.

(35) Perdew, J. P.; Wang, Y. *Phys. Rev. B* **1992**, *98*, 1372.

(36) Lee, C.; Yang, W.; Parr, R. G. *Phys. Rev. B* **1988**, *37*, 785.

(37) Perdew, J. P. *Phys. Rev. B* **1986**, *33*, 8822.

(38) Perdew, J. P.; Burke, K.; Ernzerhof, M. *Phys. Rev. Lett.* **1996**, *77*, 3865.

(39) Gill, P. M. W. *Mol. Phys.* **1996**, *89*, 433.

(40) Hamprecht, F. A.; Cohen, A. J.; Tozer, D. J.; Handy, N. C. *J. Chem. Phys.* **1998**, *109*, 6264.

(41) Adamo, C.; Barone, V. *J. Chem. Phys.* **1998**, *108*, 664.

(42) Handy, N. C.; Cohen, A. J. *Mol. Phys.* **2001**, *99*, 403.
(43) Xu, X.; Goddart, W. A. I. *Proc. Natl. Acad. Sci.* **2004**, *101*, 2673.
(44) Stephens, P. J.; Devlin, F. J.; Chabalowski, C. F.; Frisch, M. J. *J. Phys. Chem.* **1994**, *98*, 11623.
(45) Wilson, P. J.; Bradley, T. J.; Tozer, D. J. *J. Chem. Phys.* **2001**, *115*, 9233.
(46) Schmider, H. L.; Becke, A. D. *J. Chem. Phys.* **1998**, *108*, 9624.
(47) Lynch, B. J.; Fast, P. L.; Harris, M.; Truhlar, D. G. *J. Phys. Chem. A* **2000**, *104*, 4811.
(48) Zhao, Y.; Truhlar, D. G. *J. Phys. Chem. A* **2004**, *108*, 6908.
(49) Hoe, W.-M.; Cohen, A. J.; Handy, N. C. *Chem. Phys. Lett.* **2001**, *341*, 319.
(50) Adamo, C.; Cossi, M.; Barone, V. *THEOCHEM* **1999**, *493*, 145.
(51) Becke, A. D. *J. Chem. Phys.* **1996**, *104*, 1040.
(52) Krieger, J. B.; Chen, J.; Iafrate, G. J.; Savin, A. In *Electron Correlations and Materials Properties*; Gonis, A., Kioussis, N., Eds.; Plenum: New York, 1999; pp 463.
(53) Tao, J.; Perdew, J. P.; Staroverov, V. N.; Scuseria, G. E. *Phys. Rev. Lett.* **2003**, *91*, 146401.
(54) Zhao, Y.; Gonzalez-Garcia, N.; Truhlar, D. G. *J. Phys. Chem. A* **2004**, in press.
(55) Van Voorhis, T.; Scuseria, G. E. *J. Chem. Phys.* **1998**, *109*, 400.
(56) Zhao, Y.; Truhlar, D. G. *J. Chem. Theory Comput.* **2005**, *submitted*.
(57) Lynch, B. J.; Zhao, Y.; Truhlar, D. G. *J. Phys. Chem. A* **2003**, *107*, 1384.
(58) Kahn, L. R.; Baybutt, P.; Truhlar, D. G. *J. Chem. Phys.* **1976**, *65*, 3826.
(59) Krauss, M.; Stevens, W. J. *Ann. Rev. Phys. Chem.* **1984**, *35*, 357.
(60) Krauss, M.; Stevens, W. J. *Annu. Rev. Phys. Chem.* **1984**, *35*, 357.
(61) Stevens, W. J.; Basch, H.; Krauss, M. *J. Chem. Phys.* **1984**, *81*, 6026.
(62) Stevens, W. J.; Krauss, M.; Basch, H.; Jasien, P. G. *Can. J. Chem.* **1992**, *70*, 612.
(63) Cundari, T. R.; Stevens, W. J. *J. Chem. Chem. Phys.* **1993**, *98*, 5555.
(64) Wachters, A. J. H. *Chem. Phys.* **1970**, *52*, 1033.
(65) Hay, P. J. *J. Chem. Phys.* **1977**, *66*, 4377.
(66) Raghavachari, K.; Trucks, G. W. *J. Chem. Phys.* **1989**, *91*, 1062.
(67) Langhoff, S. R.; Pettersson, G. M. L.; Bauschlicher, C. W., Jr.; Partridge, H. *J. Chem. Phys.* **1987**, *86*, 268.
(68) Wadt, W. R.; Hay, P. J. *J. Chem. Phys.* **1985**, *82*, 284.
(69) Eichkorn, K.; Weigend, F.; Treutler, O.; Ahlrichs, R. *Theor. Chem. Acc.* **1997**, *97*, 119.
(70) Moore, C. E. *Atomic Energy Levels*; National Bureau of Standards, U.S. Government Printing Office: Washington DC, 1949; Vol. I-III.
(71) Herzberg, G. *Spectra of Diatomic Molecules*, 2nd ed.; D. Van Nostrand Company, Inc.: Princeton, New Jersey, 1950.
(72) Balasubramanian, K. *J. Phys. Chem.* **1989**, *93*, 6585.
(73) Spain, E. M.; Morse, M. D. *J. Chem. Phys.* **1992**, *97*, 4641.
(74) Becke, A. D. *J. Chem. Phys.* **2002**, *117*, 6935.
(75) Baerends, E. J.; Branchadell, V.; Sodupe, M. *Chem. Phys. Lett.* **1997**, *265*, 481.

(76) Reed, A. E.; Curtiss, L. A.; Weinhold, F. *Chem. Rev.* **1988**, *88*, 899.
(77) Kelloe, V.; Sadlej, A. *J. Chem. Phys.* **1995**, *103*, 2991.
(78) Langridge-Smith, P. R. R.; Morse, M. D.; Hansen, G. P.; Smalley, R. E. *J. Chem. Phys.* **1984**, *80*, 593.
(79) Balasubramanian, K.; Ravimohan, C. *J. Chem. Phys.* **1990**, *92*, 3659.
(80) Bauschlicher, C. W. J.; Partridge, H.; Langhoff, S. R.; Rosi, M. *J. Chem. Phys.* **1991**, *95*, 1057.
(81) Van Zee, R. J.; Weltner, W. J. *J. Chem. Phys.* **1995**, *103*, 2762.
(82) Diaconu, C. V.; Cho, A. E.; Doll, J. D.; Freeman, D. L. *J. Chem. Phys.* **2004**, *121*, 10026.
(83) Bauschlicher, C. W. J.; Partridge, H.; Langhoff, S. R. *Chem. Phys. Lett.* **1992**, *195*, 360.
(84) Boudreaux, E. A.; Baxter, E. *Int. J. Quantum Chemistry* **2001**, *85*, 509.
(85) Delley, B.; Freeman, A. J.; Ellis, D. E. *Phys. Rev. Lett.* **1983**, *50*, 488.
(86) Boudreaux, E. A.; Baxter, E. *Int. J. Quantum Chemistry* **2004**, *100*, 1170.
(87) Baykara, N. A.; McMaster, B. N.; Salahub, D. R. *Mol. Phys.* **1984**, *52*, 891.
(88) Goodgame, M. M.; Goddard, W. A., III. *Phys. Rev. Lett.* **1985**, *54*, 661.
(89) Roos, B. O. *Collect. Czech. Chem. Commun.* **2003**, *68*, 265.
(90) Bauschlicher, C. W. J.; Partridge, H. *Chem. Phys. Lett.* **1994**, *231*, 277.
(91) Desmarais, N.; Reuse, F. A.; Khanna, S. N. *J. Chem. Phys.* **2000**, *112*, 5576.
(92) Balasubramanian, K.; Zhu, K. *J. Chem. Phys.* **2002**, *117*, 4861.
(93) Langhoff, S. R.; Bauschlicher, C. W. J. *J. Chem. Phys.* **1986**, *84*, 4485.
(94) Sunil, K. K.; Jordan, K. D.; Raghavachari, K. *J. Phys. Chem.* **1985**, *89*, 457.
(95) Lynch, B. J.; Truhlar, D. G. *J. Phys. Chem. A* **2003**, *107*, 8996.
(96) Perdew, J. P.; Schmidt, K. *AIP Conference Proceedings* **2001**, *577*, 1.
(97) Staroverov, V. N.; Scuseria, G. E.; Tao, J.; Perdew, J. P. *Phys. Rev. B* **2004**, *69*, 075102.
(98) Genesis 28: 12-15.
(99) Fuchs, M.; Bockstedten, M.; Pehlke, E.; Scheffler, M. *Phys. Rev. B* **1998**, *51*, 2134.

Table 1: Experimental data[a] used for TMAE9/05 and TMBL8/05

	D_0	ω_e	$x_e\omega_e$	D_e	r_e[b]	References
Ag_2	38.0 ± 0.7	192.4	1.6	38.3	2.53	20, 21, 26
AgCu	40.7 ± 2.3	231.0	0.9	40.9	2.37	26, 27
Cr_2	35.3 ± 1.4	480.6	14.1	36.0	1.68	20, 29
Cu_2	46.8 ± 0.5	266.5	1.0	47.2	2.22	20, 26
Mo_2	103.2 ± 0.2	477.1	1.5	103.9	1.93	20
Ni_2[c]	47.1 ± 0.2	259.2	1.9	47.6	2.15	20, 22
V_2	63.4 ± 0.1	536.9	4.1	64.2	1.77	20
Zr_2[d]	70.4 ± 0.0	305.7	0.5	70.8	2.24	20, 24
ZrV[e]	61.4 ± 0.1			61.9		28

[a] D_0, D_e in kcal/mol; ω_e, $x_e\omega_e$ in cm^{-1}; r_e in Å

[b] experimental uncertainties for the bond lengths are not given because they are smaller than the accuracy in which we quote the numbers

[c] Ref. 20 reports r_0 (although it is denoted as r_e) for Ni_2 and we have converted this value to an r_e using the data is ref. 20 and 72.

[d] Ref. 20 reports the r_0 for Zr_2 and we have converted this value to an r_e using the data is ref. 24.

[e] The zero point energy was calculated with B3LYP/DZQ and scaled by 0.983. The harmonic frequency using B3LYP/DZQ for ZrV is 325.5 cm^{-1}.

Table 2: Summary of the DFT methods used in this paper where HGGA stands for hybrid GGA, MGGA stands for meta GGA, HMGGA stands for hybrid meta GGA, and LSDA stands for local spin density approximation.

	X	Type	exchange functional	correlation functional
B1B95	28	HMGGA	Becke88	Becke95
B3LYP	20	HGGA	Becke88	Lee-Yang-Parr
B3P86	20	HGGA	Becke88	Perdew86
B3PW91	20	HGGA	Becke88	Perdew-Wang91
B97-1	21	HGGA	B97-1	B97-1
B97-2	21	HGGA	B97-2	B97-2
B98	21.98	HGGA	B98	B98
BB1K	42	HMGGA	Becke88	Becke95
BB95		MDFT	Becke88	Becke95
BH&HLYP	50	HGGA	Becke88	Lee-Yang-Parr
BLYP		GGA	Becke88	Lee-Yang-Parr
BP86		GGA	Becke88	Perdew86
BPBE		GGA	Becke88	Perdew-Burke-Ernzerhof
BPW91		GGA	Becke88	Perdew-Wang91
G96LYP		GGA	Gill96	Lee-Yang-Parr
HCTH		GGA	Hamprecht-Cohen-Tozer-Handy	Hamprecht-Cohen-Tozer-Handy
mPW1B95	31	HMGGA	modified Perdew-Wang91	Becke95
MPW1K	42.8	HGGA	modified Perdew-Wang91	Perdew-Wang91
mPW1PW91	25	HGGA	modified Perdew-Wang91	Perdew-Wang91
MPW3LYP	21.8	HGGA	modified Perdew-Wang91	Lee-Yang-Parr
mPWB95		MDFT	modified Perdew-Wang91	Becke95
MPW1KCIS	15	HMGGA	modified Perdew-Wang91	Krieger-Chen-InfanteSavin
MPWKCIS		MDFT	modified Perdew-Wang91	Krieger-Chen-Infante-Savin
MPWKCIS1K	41	HMGGA	modified Perdew-Wang91	Krieger-Chen-Infante-Savin
mPWLYP		GGA	modified Perdew-Wang91	Lee-Yang-Parr
mPWPBE		GGA	modified Perdew-Wang91	Perdew-Burke-Ernzerhof
mPWPW91		GGA	modified Perdew-Wang91	Perdew-Wang91
O3LYP	11.61	HGGA	OPTX	Lee-Yang-Parr
OLYP		GGA	OPTX	Lee-Yang-Parr
PBE		GGA	Perdew-Burke-Ernzerhof	Perdew-Burke-Ernzerhof
PBE1KCIS	22	HMGGA	Perdew-Burke-Ernzerhof	Krieger-Chen-Infante-Savin
PBE1PBE	25	HGGA	Perdew-Burke-Ernzerhof	Perdew-Burke-Ernzerhof
PBEKCIS		MGGA	Perdew-Burke-Ernzerhof	Krieger-Chen-Infante-Savin
SVWN3		LSDA	Slater	VWN no. 3
SPWL		LSDA	Slater	Perdew-Wang local
TPSS		MDFT	Tao-Perdew-Staroverov-Scuseria	Tao-Perdew-Staroverov-Scuseria
TPSS1KCIS	13	HMGGA	Tao-Perdew-Staroverov-Scuseria	Krieger-Chen-Infante-Savin
TPSSh	10	HMGGA	Tao-Perdew-Staroverov-Scuseria	Tao-Perdew-Staroverov-Scuseria
TPSSKCIS		MDFT	Tao-Perdew-Staroverov-Scuseria	Krieger-Chen-Infante-Savin
VSXC		MDFT	van Voorhis-Scuseria	van Voorhis-Scuseria
X3LYP	21.8	HGGA	Becke88 + Perdew-Wang91	Lee-Yang-Parr
XLYP		GGA	Becke88 + Perdew-Wang91	Lee-Yang-Parr

Table 3: Experimental spin-orbit energies (ΔE_{SO})[a] given in kcal/mol[a]

	ΔE_{SO}
Ag_2, AgCu, Cr_2, Cu_2, Mo_2	0.00
Ni_2	–5.56
V_2	–1.83
Zr_2	–3.30
ZrV	–2.98

[a] $\Delta E_{SO} \equiv E_{SO}(A) + E_{SO}(B) - E_{SO}(AB)$, where $E_{SO}(A)$ and $E_{SO}(B)$ are the spin-orbit energies of atoms A and B and $E_{SO}(AB)$ is the spin-orbit energy of the diatomic molecule AB.

Table 4: Atomic ground states for Ni, V, and Zr.

	Ni		V		Zr	
	DZQ	TZQ	DZQ	TZQ	DZQ	TZQ
HF	$4s^{2.0}3d^{8.0}$	$4s^{2.0}3d^{8.0}$	$4s^{2.0}3d^{3.0}$	$4s^{2.0}3d^{3.0}$	$5s^{2.0}4d^{2.0}$	$5s^{2.0}4d^{2.0}$
			LSDA			
SPWL	$4s^{1.3}3d^{8.7}$	$4s^{1.0}3d^{9.0}$	$4s^{1.0}3d^{4.0}$	$4s^{1.0}3d^{4.0}$	$5s^{1.0}4d^{3.0}$	$5s^{1.0}4d^{3.0}$
SVWN3	$4s^{1.2}3d^{8.8}$	$4s^{1.0}3d^{9.0}$	$4s^{1.0}3d^{4.0}$	$4s^{1.0}3d^{4.0}$	$5s^{2.0}4d^{2.0}$	$5s^{2.0}4d^{2.0}$
			GGA			
BLYP	$4s^{1.4}3d^{8.6}$	$4s^{1.2}3d^{8.8}$	$4s^{1.0}3d^{4.0}$	$4s^{1.0}3d^{4.0}$	$5s^{2.0}4d^{2.0}$	$5s^{2.0}4d^{2.0}$
BP86	$4s^{1.3}3d^{8.7}$	$4s^{1.1}3d^{8.9}$	$4s^{1.0}3d^{4.0}$	$4s^{1.0}3d^{4.0}$	$5s^{1.0}4d^{3.0}$	$5s^{1.0}4d^{3.0}$
BPBE	$4s^{1.3}3d^{8.7}$	$4s^{1.1}3d^{8.9}$	$4s^{1.0}3d^{4.0}$	$4s^{1.0}3d^{4.0}$	$5s^{1.0}4d^{3.0}$	$5s^{1.0}4d^{3.0}$
BPW91	$4s^{1.3}3d^{8.7}$	$4s^{1.1}3d^{8.9}$	$4s^{1.0}3d^{4.0}$	$4s^{1.0}3d^{4.0}$	$5s^{1.0}4d^{3.0}$	$5s^{1.0}4d^{3.0}$
G96LYP	$4s^{1.4}3d^{8.6}$	$4s^{1.1}3d^{8.9}$	$4s^{1.0}3d^{4.0}$	$4s^{1.0}3d^{4.0}$	$5s^{2.0}4d^{2.0}$	$5s^{2.0}4d^{2.0}$
HCTH	$4s^{1.3}3d^{8.7}$	$4s^{1.2}3d^{8.8}$	$4s^{2.0}3d^{3.0}$	$4s^{1.0}3d^{4.0}$	$5s^{2.0}4d^{2.0}$	$5s^{2.0}4d^{2.0}$
mPWLYP	$4s^{1.4}3d^{8.6}$	$4s^{1.2}3d^{8.8}$	$4s^{1.0}3d^{4.0}$	$4s^{1.0}3d^{4.0}$	$5s^{2.0}4d^{2.0}$	$5s^{2.0}4d^{2.0}$
mPWPBE	$4s^{1.3}3d^{8.7}$	$4s^{1.1}3d^{8.9}$	$4s^{1.0}3d^{4.0}$	$4s^{1.0}3d^{4.0}$	$5s^{1.0}4d^{3.0}$	$5s^{1.0}4d^{3.0}$
mPWPW91	$4s^{1.3}3d^{8.7}$	$4s^{1.0}3d^{9.0}$	$4s^{1.0}3d^{4.0}$	$4s^{1.0}3d^{4.0}$	$5s^{1.0}4d^{3.0}$	$5s^{1.0}4d^{3.0}$
OLYP	$4s^{1.2}3d^{8.8}$	$4s^{1.1}3d^{8.9}$	$4s^{1.0}3d^{4.0}$	$4s^{1.0}3d^{4.0}$	$5s^{1.0}4d^{3.0}$	$5s^{1.0}4d^{3.0}$
PBE	$4s^{1.3}3d^{8.7}$	$4s^{1.2}3d^{8.8}$	$4s^{1.0}3d^{4.0}$	$4s^{1.0}3d^{4.0}$	$5s^{1.0}4d^{3.0}$	$5s^{1.0}4d^{3.0}$
XLYP	$4s^{1.4}3d^{8.6}$	$4s^{1.0}3d^{9.0}$	$4s^{1.0}3d^{4.0}$	$4s^{1.0}3d^{4.0}$	$5s^{2.0}4d^{2.0}$	$5s^{2.0}4d^{2.0}$
			hybrid GGA			
B3LYP	$4s^{1.0}3d^{9.0}$	$4s^{1.0}3d^{9.0}$	$4s^{2.0}3d^{3.0}$	$4s^{1.0}3d^{4.0}$	$5s^{2.0}4d^{2.0}$	$5s^{2.0}4d^{2.0}$
B3P86	$4s^{1.0}3d^{9.0}$	$4s^{1.0}3d^{9.0}$	$4s^{1.0}3d^{4.0}$	$4s^{1.0}3d^{4.0}$	$5s^{2.0}4d^{2.0}$	$5s^{2.0}4d^{2.0}$
B3PW91	$4s^{1.0}3d^{9.0}$	$4s^{1.0}3d^{9.0}$	$4s^{1.0}3d^{4.0}$	$4s^{1.0}3d^{4.0}$	$5s^{1.0}4d^{3.0}$	$5s^{1.0}4d^{3.0}$
B97-1	$4s^{2.0}3d^{8.0}$	$4s^{1.0}3d^{9.0}$	$4s^{2.0}3d^{3.0}$	$4s^{2.0}3d^{3.0}$	$5s^{2.0}4d^{2.0}$	$5s^{2.0}4d^{2.0}$
B97-2	$4s^{1.1}3d^{8.9}$	$4s^{1.0}3d^{9.0}$	$4s^{2.0}3d^{3.0}$	$4s^{1.0}3d^{4.0}$	$5s^{2.0}4d^{2.0}$	$5s^{2.0}4d^{2.0}$
B98	$4s^{2.0}3d^{8.0}$	$4s^{1.0}3d^{9.0}$	$4s^{2.0}3d^{3.0}$	$4s^{2.0}3d^{3.0}$	$5s^{2.0}4d^{2.0}$	$5s^{2.0}4d^{2.0}$
BH&HLYP	$4s^{1.0}3d^{9.0}$	$4s^{1.0}3d^{9.0}$	$4s^{2.0}3d^{3.0}$	$4s^{2.0}3d^{3.0}$	$5s^{2.0}4d^{2.0}$	$5s^{2.0}4d^{2.0}$
MPW1K	$4s^{1.0}3d^{9.0}$	$4s^{1.0}3d^{9.0}$	$4s^{1.0}3d^{4.0}$	$4s^{1.0}3d^{4.0}$	$5s^{1.0}4d^{3.0}$	$5s^{1.0}4d^{3.0}$
MPW1PW91	$4s^{1.0}3d^{9.0}$	$4s^{1.0}3d^{9.0}$	$4s^{1.0}3d^{4.0}$	$4s^{1.0}3d^{4.0}$	$5s^{1.0}4d^{3.0}$	$5s^{1.0}4d^{3.0}$
MPW3LYP	$4s^{1.1}3d^{8.9}$	$4s^{1.0}3d^{9.0}$	$4s^{2.0}3d^{3.0}$	$4s^{1.0}3d^{4.0}$	$5s^{2.0}4d^{2.0}$	$5s^{2.0}4d^{2.0}$
O3LYP	$4s^{1.0}3d^{9.0}$	$4s^{1.0}3d^{9.0}$	$4s^{1.0}3d^{4.0}$	$4s^{1.0}3d^{4.0}$	$5s^{2.0}4d^{2.0}$	$5s^{2.0}4d^{2.0}$
PBE1PBE	$4s^{1.1}3d^{8.9}$	$4s^{1.0}3d^{9.0}$	$4s^{1.0}3d^{4.0}$	$4s^{1.0}3d^{4.0}$	$5s^{1.0}4d^{3.0}$	$5s^{1.0}4d^{3.0}$
X3LYP	$4s^{1.1}3d^{8.9}$	$4s^{1.0}3d^{9.0}$	$4s^{2.0}3d^{3.0}$	$4s^{2.0}3d^{3.0}$	$5s^{2.0}4d^{2.0}$	$5s^{2.0}4d^{2.0}$
			meta GGA			
BB95	$4s^{2.0}3d^{8.0}$	$4s^{1.0}3d^{9.0}$	$4s^{1.0}3d^{4.0}$	$4s^{1.0}3d^{4.0}$	$5s^{2.0}4d^{2.0}$	$5s^{2.0}4d^{2.0}$
mPWB95	$4s^{2.0}3d^{8.0}$	$4s^{1.0}3d^{9.0}$	$4s^{1.0}3d^{4.0}$	$4s^{1.0}3d^{4.0}$	$5s^{2.0}4d^{2.0}$	$5s^{2.0}4d^{2.0}$
mPWKCIS	$4s^{1.3}3d^{8.7}$	$4s^{1.0}3d^{9.0}$	$4s^{1.0}3d^{4.0}$	$4s^{1.0}3d^{4.0}$	$5s^{1.0}4d^{3.0}$	$5s^{1.0}4d^{3.0}$
PBEKCIS	$4s^{1.3}3d^{8.7}$	$4s^{2.0}3d^{8.0}$	$4s^{1.0}3d^{4.0}$	$4s^{1.0}3d^{4.0}$	$5s^{2.0}4d^{2.0}$	$5s^{2.0}4d^{2.0}$
TPSSKCIS	$4s^{1.3}3d^{8.7}$	$4s^{1.1}3d^{8.9}$	$4s^{1.0}3d^{4.0}$	$4s^{1.0}3d^{4.0}$	$5s^{1.0}4d^{3.0}$	$5s^{1.0}4d^{3.0}$
TPSS	$4s^{1.3}3d^{8.7}$	$4s^{1.2}3d^{8.8}$	$4s^{1.0}3d^{4.0}$	$4s^{1.0}3d^{4.0}$	$5s^{2.0}4d^{2.0}$	$5s^{2.0}4d^{2.0}$
VSXC	$4s^{1.3}3d^{8.7}$	$4s^{1.3}3d^{8.7}$	$4s^{2.0}3d^{3.0}$	$4s^{1.0}3d^{4.0}$	$5s^{2.0}4d^{2.0}$	$5s^{2.0}4d^{2.0}$
			hybrid meta GGA			
B1B95	$4s^{1.1}3d^{8.9}$	$4s^{1.0}3d^{9.0}$	$4s^{1.0}3d^{4.0}$	$4s^{1.0}3d^{4.0}$	$5s^{2.0}4d^{2.0}$	$5s^{2.0}4d^{2.0}$
BB1K	$4s^{1.0}3d^{9.0}$	$4s^{1.0}3d^{9.0}$	$4s^{1.0}3d^{4.0}$	$4s^{1.0}3d^{4.0}$	$5s^{2.0}4d^{2.0}$	$5s^{2.0}4d^{2.0}$
MPW1B95	$4s^{2.0}3d^{8.0}$	$4s^{2.0}3d^{8.0}$	$4s^{1.0}3d^{4.0}$	$4s^{1.0}3d^{4.0}$	$5s^{2.0}4d^{2.0}$	$5s^{2.0}4d^{2.0}$
MPW1KCIS	$4s^{1.0}3d^{9.0}$	$4s^{1.0}3d^{9.0}$	$4s^{1.0}3d^{4.0}$	$4s^{1.0}3d^{4.0}$	$5s^{1.0}4d^{3.0}$	$5s^{1.0}4d^{3.0}$
MPWKCIS1K	$4s^{2.0}3d^{8.0}$	$4s^{1.0}3d^{9.0}$	$4s^{1.0}3d^{4.0}$	$4s^{1.0}3d^{4.0}$	$5s^{2.0}4d^{2.0}$	$5s^{1.0}4d^{3.0}$
PBE1KCIS	$4s^{2.0}3d^{8.0}$	$4s^{1.0}3d^{9.0}$	$4s^{1.0}3d^{4.0}$	$4s^{1.0}3d^{4.0}$	$5s^{2.0}4d^{2.0}$	$5s^{2.0}4d^{2.0}$
TPSSh	$4s^{1.0}3d^{9.0}$	$4s^{1.0}3d^{9.0}$	$4s^{1.0}3d^{4.0}$	$4s^{1.0}3d^{4.0}$	$5s^{1.0}4d^{3.0}$	$5s^{2.0}4d^{2.0}$

TPSS1KCIS	$4s^{2.0}3d^{8.0}$	$4s^{1.0}3d^{9.0}$	$4s^{1.0}3d^{4.0}$	$4s^{1.0}3d^{4.0}$	$5s^{1.0}4d^{3.0}$	$5s^{1.0}4d^{3.0}$

Table 5: Ground states for Ni_2

	DZQ	TZQ		DZQ	TZQ
	LSDA			*hybrid GGA*	
SPWL	$^3\Sigma_g^-$	$^3\Sigma_g^-$	B3LYP	$^3\Pi_u$	$^3\Pi_u$
SVWN3	$^3\Sigma_g^-$	$^3\Sigma_g^-$	B3P86	$^3\Pi_u$	$^3\Pi_u$
	GGA		B3PW91	$^3\Pi_u$	$^3\Pi_u$
BLYP	$^3\Pi_u$	$^3\Pi_u$	B97-1	$^3\Pi_u$	$^3\Pi_u$
BP86	$^3\Pi_u$	$^3\Pi_u$	B97-2	$^3\Pi_u$	$^3\Pi_u$
BPBE	$^3\Pi_u$	$^3\Pi_u$	B98	$^3\Pi_u$	$^3\Pi_u$
BPW91	$^3\Pi_u$	$^3\Pi_u$	BH&HLYP	$^3\Pi_u$	$^3\Pi_u^+$
G96LYP	$^3\Pi_u$	$^3\Pi_u$	MPW1K	$^3\Pi_u$	$^3\Pi_u^+$
HCTH	$^3\Pi_u$	$^3\Pi_u$	mPW1PW91	$^3\Pi_u$	$^3\Pi_u$
mPWLYP	$^3\Pi_u$	$^3\Pi_u$	MPW3LYP	$^3\Pi_u$	$^3\Pi_u$
mPWPBE	$^3\Pi_u$	$^3\Pi_u$	O3LYP	$^3\Pi_u$	$^3\Pi_u$
mPWPW91	$^3\Pi_u$	$^3\Pi_u$	PBE0	$^3\Pi_u$	$^3\Pi_u$
OLYP	$^3\Pi_u$	$^3\Pi_u$	X3LYP	$^3\Pi_u$	$^3\Pi_u$
PBE	$^3\Pi_u$	$^3\Pi_u$	*hybrid meta GGA*		
XLYP	$^3\Pi_u$	$^3\Pi_u$	B1B95	$^3\Pi_u$	$^3\Pi_u$
meta GGA			BB1K	$^3\Pi_u$	$^3\Pi_u^+$
BB95	$^3\Pi_u$	$^3\Pi_u$	MPW1B95	$^3\Pi_u^+$	$^3\Pi_u^+$
mPWB95	$^3\Pi_u$	$^3\Pi_u$	MPW1KCIS	$^3\Pi_u$	$^3\Pi_u$
MPWKCIS	$^3\Pi_u$	$^3\Pi_u$	MPWKCIS1K	$^3\Pi_u^+$	$^3\Pi_u$
PBEKCIS	$^3\Pi_u$	$^3\Pi_u$	PBE1KCIS	$^3\Pi_u^+$	$^3\Pi_u$
TPSSKCIS	$^3\Pi_u$	$^3\Pi_u$	TPSSh	$^3\Pi_u$	$^3\Pi_u$
TPSS	$^3\Pi_u$	$^3\Pi_u$	TPSS1KCIS	$^3\Pi_u$	$^3\Pi_u$
VSXC	$^3\Pi_u$	$^3\Pi_u$			

Table 6: Atomization energies (kcal/mol) for the dimers in TMAE9/05: mean signed errors (MSEs), mean unsigned errors (MUEs), root-mean-square errors (RMSEs), and the average mean unsigned errors (AMUEs) for the atomization energies

	MSE	MUE	RMSE	MSE	MUE	RMSE	AMUE[a]
	DZQ			TZQ			
HF	-54.2	54.2	59.0	-53.5	53.5	58.2	53.9
			LSDA				
SVWN3	24.9	24.9	26.8	32.7	32.7	35.5	28.8
SPWL	21.6	21.6	23.6	28.0	28.0	30.2	24.8
average	*23.3*	*23.3*		*30.4*	*30.4*		*26.8*
			GGA				
BLYP	-1.7	3.4	5.3	4.8	5.3	7.4	4.3
BP86	-0.4	7.1	9.9	5.6	7.6	9.6	7.4
BPBE	-7.7	8.5	14.4	-2.9	6.2	9.5	7.4
BPW91	-8.3	9.0	15.9	-2.9	6.1	9.5	7.6
G96LYP	-6.3	6.3	9.9	0.2	4.8	5.5	5.6
HCTH	6.8	8.7	10.4	11.3	11.9	15.4	10.3
mPWLYP	1.1	3.3	4.4	7.7	7.7	10.0	5.6
mPWPBE	-4.6	7.7	12.2	0.5	6.5	8.6	7.1
mPWPW91	-5.1	8.1	13.6	0.5	6.4	8.6	7.3
OLYP	-7.1	8.6	13.3	-2.8	7.7	9.2	8.1
PBE	-0.8	7.8	10.8	3.9	7.7	9.3	7.8
XLYP	-0.6	3.7	5.0	6.4	6.5	8.8	5.1
average	*-2.9*	*6.9*		*2.7*	*7.1*		*7.0*
			hybrid GGA				
B3LYP	-20.6	20.6	27.0	-16.7	16.7	20.5	18.6
B3P86	-18.4	18.4	26.5	-14.8	14.9	20.7	16.6
B3PW91	-24.3	24.3	32.9	-21.1	21.1	27.2	22.7
B97-1	-18.6	20.6	28.4	-6.8	8.5	11.2	14.6
B97-2	-11.9	13.6	19.6	-3.6	5.3	7.8	9.4
B98	-19.0	20.2	28.2	-8.9	9.7	13.1	15.0
BH&HLYP	-38.6	38.6	46.4	-37.7	37.7	45.0	38.2
MPW1K	-34.1	34.1	41.9	-31.8	31.8	39.5	33.0
mPW1PW91	-26.4	26.4	35.2	-25.2	25.2	32.7	25.8
MPW3LYP	-20.6	20.6	27.9	-16.0	16.0	20.2	18.3
O3LYP	-16.7	16.7	21.9	-12.7	13.4	16.3	15.1
PBE1PBE	-24.8	24.8	34.0	-19.3	25.0	31.6	24.9
X3LYP	-20.6	20.6	28.0	-17.4	17.4	21.6	19.0
average	*-22.7*	*23.0*		*-17.9*	*18.7*		*20.9*
			meta GGA				
BB95	7.0	12.4	17.4	9.5	9.5	12.3	11.0
mPWB95	9.9	13.1	18.1	13.0	13.0	15.5	13.0
mPWKCIS	-4.1	6.6	11.3	1.5	6.0	7.7	6.3
PBEKCIS	-1.1	6.1	8.8	5.1	7.3	9.2	6.7
TPSSKCIS	-5.6	7.1	12.4	-0.6	5.9	8.9	6.5
TPSS	-6.1	8.5	13.7	-1.3	6.1	10.0	7.3

VSXC	4.3	11.4	15.4	5.5	10.2	11.2	10.8
average	*0.6*	*9.3*		*4.7*	*8.3*		*8.8*
			hybrid meta GGA				
B1B95	-24.0	24.0	32.4	-21.9	21.9	29.1	22.9
BB1K	-30.1	30.1	38.2	-27.8	27.8	35.8	29.0
MPW1B95	-23.0	23.0	32.4	-20.7	20.7	28.5	21.8
MPW1KCIS	-19.0	19.0	25.5	-15.4	15.4	20.1	17.2
MPWKCIS1K	-34.1	34.1	41.1	-31.7	31.7	39.1	32.9
PBE1KCIS	-23.3	23.3	31.3	-20.4	20.4	26.3	21.9
TPSSh	-15.3	15.5	23.0	-11.0	11.0	16.4	13.2
TPSS1KCIS	-18.2	18.2	24.9	-12.0	12.0	16.4	15.1
average	*-23.4*	*23.4*		*-20.1*	*20.1*		*21.8*

[a] The AMUE denotes average mean unsigned error and is the average of the MUEs with the DZQ and TZQ basis levels.

Table 7: Atomization energies: Mean unsigned errors (in kcal/mol) for three databases.[a]

	AE6	BH6	TMAE9/05
		LSDA	
SVWN3	17.38	18.17	32.7
SPWL	15.97	17.97	28.0
average	*16.68*	*18.07*	*30.4*
		GGA	
BLYP	1.31	7.83	5.3
BP86	3.48	9.29	7.6
BPBE	1.42	7.53	6.2
BPW91	1.35	7.44	6.1
G96LYP	1.65	6.60	4.8
HCTH	1.08	5.25	11.9
mPWLYP	1.49	8.85	7.7
mPWPBE	2.07	8.56	6.5
mPWPW91	2.19	8.47	6.4
OLYP	0.79	5.87	7.7
PBE	3.20	9.33	7.7
XLYP	1.26	8.34	6.5
average	*1.77*	*7.78*	*7.1*
		hybrid GGA	
B3LYP	0.61	4.73	16.7
B3P86	3.30	6.02	14.9
B3PW91	0.63	4.41	21.1
B97-1	0.81	4.14	8.5
B97-2	0.82	3.21	5.3
B98	0.50	4.00	9.7
BH&HLYP	4.20	1.98	37.7
MPW1K	2.18	1.40	31.8
mPW1PW91	0.91	3.95	25.2
MPW3LYP	0.43	5.27	16.0
O3LYP	0.64	4.45	13.4
PBE1PBE	1.23	4.62	25.0
X3LYP	0.99	4.22	17.4
average	*1.33*	*4.03*	*18.7*
		meta GGA	
BB95	2.56	8.02	9.5
mPWB95	3.42	9.17	13.0
mPWKCIS	1.56	7.56	6.0

PBEKCIS	2.38	8.33	7.3
TPSSKCIS	1.15	7.08	5.9
TPSS	1.24	8.30	6.1
VSXC	0.70	4.98	10.2
average	*1.86*	*7.63*	*8.3*
	hybrid meta GGA		
B1B95	0.60	3.14	21.9
BB1K	1.20	1.14	27.8
MPW1B95	0.87	3.38	20.7
MPW1KCIS	0.68	4.73	15.4
MPWKCIS1K	2.34	1.20	31.7
PBE1KCIS	0.73	4.09	20.4
TPSSh	1.39	6.72	11.0
TPSS1KCIS	0.79	4.98	12.0
average	*1.08*	*3.67*	*20.1*

[a] The results for AE6 and BH6 are based on the MG3S basis, and those for TMAE9/05 are based on the comparable TZQ database. The results are "per bond" for AE6 and TMAE9/5 (in the latter case obviously so since all molecules in the latter set have only one bond).

Table 8: Atomization energies (kcal/mol) for Ag_2, CuAg, Cu_2, Cr_2, and Mo_2: The mean signed errors (MSEs), mean unsigned errors (MUEs), root-mean-square errors (RMSEs), and the average mean unsigned errors (AMUEs)

	MSE	MUE	RMSE	MSE	MUE	RMSE	AMUE[a]
	DZQ			TZQ			
HF	-46.0	46.0	53.8	-46.7	46.7	53.9	46.4
			LSDA				
SVWN3	16.3	16.3	16.4	23.5	23.5	25.8	19.9
SPWL	13.5	13.5	13.8	20.2	20.2	27.7	16.9
average	*14.9*	*14.9*		*21.9*	*21.9*		*18.4*
			GGA				
BLYP	-2.4	4.7	6.9	1.5	2.4	4.0	3.5
BP86	-4.5	8.3	11.9	-0.5	3.3	4.6	5.8
BPBE	-10.2	11.0	17.8	-8.1	8.1	12.2	9.6
BPW91	-11.3	12.1	20.1	-8.0	8.0	12.1	10.1
G96LYP	-7.9	7.9	12.3	-4.1	4.1	5.2	6.0
HCTH	3.6	7.0	9.8	4.8	6.0	9.8	6.5
mPWLYP	0.6	4.3	5.2	4.5	4.5	6.7	4.4
mPWPBE	-7.5	10.1	15.4	-5.1	5.7	9.2	7.9
mPWPW91	-8.4	11.0	17.4	-5.1	5.6	9.2	8.3
OLYP	-12.0	12.0	17.1	-9.4	9.4	10.5	10.7
PBE	-5.2	9.6	13.3	-2.3	4.6	6.8	7.1
XLYP	-2.7	4.3	6.1	2.9	3.1	5.2	3.7
average	*-5.7*	*8.5*		*-2.4*	*5.4*		*7.0*
			hybrid GGA				
B3LYP	-13.2	13.2	21.3	-11.6	11.6	16.4	12.4
B3P86	-13.9	13.9	23.7	-12.1	12.1	18.5	13.0
B3PW91	-18.5	18.5	28.9	-17.0	17.0	24.3	17.8
B97-1	-6.6	10.2	18.7	-1.2	4.2	6.1	7.2
B97-2	-6.6	9.6	18.2	-0.6	3.6	5.1	6.6
B98	-5.7	7.8	14.2	-3.4	4.9	8.3	6.3
BH&HLYP	-23.4	23.4	34.3	-23.0	23.0	32.6	23.2
MPW1K	-25.1	25.1	37.0	-24.6	24.6	35.2	24.9
mPW1PW91	-19.8	19.8	31.1	-18.5	18.5	26.9	19.1
MPW3LYP	-11.1	11.1	19.5	-9.6	9.6	14.5	10.4
O3LYP	-15.2	15.2	21.4	-13.4	13.4	16.5	14.3
PBE1PBE	-18.5	18.5	29.9	-16.9	16.9	25.4	17.7
X3LYP	-14.4	14.4	22.4	-11.3	11.3	16.4	12.8
average	*-14.7*	*15.4*		*-12.6*	*13.1*		*14.3*
			meta GGA				
BB95	-2.5	7.2	8.4	3.0	3.0	3.7	5.1
mPWB95	0.6	6.3	6.6	6.1	6.1	6.8	6.2
mPWKCIS	-7.5	8.9	14.6	-4.1	4.2	6.9	6.5
PBEKCIS	-4.5	7.5	11.0	-0.9	3.1	4.6	5.3
TPSSKCIS	-8.1	9.1	15.4	-5.8	6.0	10.6	7.6
TPSS	-7.5	10.2	16.1	-6.1	7.4	12.6	8.8

VSXC	1.6	14.2	16.8	3.2	11.5	12.1	12.9
average	*-4.0*	*9.1*		*-0.6*	*5.9*		*7.5*
			hybrid meta GGA				
B1B95	-17.8	17.8	28.4	-16.1	16.1	24.1	16.9
BB1K	-22.6	22.6	34.8	-20.8	20.8	30.6	21.7
MPW1B95	-17.1	17.1	28.4	-14.9	14.9	22.9	16.0
MPW1KCIS	-15.4	15.4	24.4	-14.0	14.0	19.7	14.7
MPWKCIS1K	-24.9	24.9	36.4	-24.1	24.1	34.2	24.5
PBE1KCIS	-17.1	17.1	27.2	-15.2	15.2	22.4	16.1
TPSSh	-12.6	12.8	22.4	-10.7	10.7	17.5	11.8
TPSS1KCIS	-14.8	14.8	24.1	-13.1	13.1	19.3	14.0
average	*-17.8*	*17.8*		*-16.1*	*16.1*		*17.0*

[a] The AMUE denotes average mean unsigned error and is the average of the MUEs with the DZQ and TZQ basis levels.

Table 9: Atomization energies (kcal/mol) for Ag_2, CuAg, Cu_2, and Zr_2: The mean signed errors (MSEs), mean unsigned errors (MUEs), root-mean-square errors (RMSEs), and the average mean unsigned errors (AMUEs)

methods	MSE	MUE	RMSE	MSE	MUE	RMSE	AMUE[a]
	DZQ			TZQ			
HF	-42.1	42.1	46.0	-43.2	43.2	46.8	42.7
LSDA							
SVWN3	21.8	21.8	23.6	22.5	18.0	25.9	19.9
SPWL	20.0	20.0	21.4	20.6	16.5	23.5	18.2
average	*20.9*	*20.9*		*21.5*	*17.2*		*19.1*
GGA							
BLYP	0.9	1.9	2.1	0.4	1.5	1.8	1.7
BP86	4.9	4.9	5.8	3.7	4.6	7.5	4.7
BPBE	0.2	0.9	1.0	0.1	2.2	2.7	1.5
BPW91	0.2	0.9	1.0	0.0	2.2	2.7	1.5
G96LYP	-1.0	1.0	1.4	-1.1	3.5	3.6	2.2
HCTH	3.7	4.7	5.9	3.1	5.3	9.0	5.0
mPWLYP	2.7	3.0	3.4	1.7	2.1	2.8	2.6
mPWPBE	2.7	2.7	2.9	2.0	2.8	4.6	2.7
mPWPW91	2.7	2.7	2.9	1.9	2.8	4.5	2.7
OLYP	-2.5	5.2	5.2	-2.0	7.9	8.1	6.5
PBE	4.9	4.9	5.4	3.9	4.9	7.0	4.9
XLYP	0.5	2.4	2.6	1.1	1.5	2.2	1.9
average	*1.6*	*2.9*		*1.2*	*3.4*		*3.2*
hybrid GGA							
B3LYP	-6.4	6.4	9.3	-6.2	6.2	7.2	6.3
B3P86	-2.4	2.4	3.1	-1.9	2.1	2.6	2.3
B3PW91	-6.4	6.4	7.6	-5.8	5.8	6.0	6.1
B97-1	-1.4	5.9	7.8	-0.3	4.1	5.0	5.0
B97-2	-0.3	3.4	4.2	1.4	1.8	2.1	2.6
B98	-2.7	5.3	8.2	-1.6	3.5	5.3	4.4
BH&HLYP	-19.2	19.2	25.9	-18.3	18.3	23.2	18.7
MPW1K	-14.3	14.3	17.4	-13.0	13.0	14.5	13.7
mPW1PW91	-7.7	7.7	9.5	-7.0	7.0	7.4	7.4
MPW3LYP	-6.0	6.0	9.7	-5.7	5.7	7.2	5.8
O3LYP	-5.8	5.8	6.0	-5.2	6.6	7.0	6.2
PBE1PBE	-6.0	6.0	7.5	3.1	9.8	13.5	7.9
X3LYP	-6.1	6.1	7.2	-6.3	6.3	7.7	6.2
average	*-6.5*	*7.3*		*-5.2*	*6.9*		*7.1*
meta GGA							
BB95	6.4	6.4	7.8	6.6	6.6	9.9	6.5
mPWB95	8.2	8.2	9.2	8.3	8.3	11.0	8.2
mPWS	2.1	2.2	2.9	1.6	3.2	4.9	2.7
PBEKCIS	3.6	3.6	4.2	4.4	4.4	7.2	4.0
TPSSKCIS	1.3	1.3	1.7	1.3	2.5	3.6	1.9
TPSS	2.3	2.3	2.4	2.3	2.3	3.3	2.3

VSXC	9.8	10.0	11.6	10.2	10.2	11.0	10.1
average	*4.8*	*4.9*		*5.0*	*5.4*		*5.1*
			hybrid GGA				
B1B95	-5.5	5.5	6.9	-4.4	4.4	4.6	4.9
BB1K	-10.7	10.7	13.7	-9.3	9.3	10.6	10.0
MPW1B95	-5.4	5.4	7.6	-4.3	4.3	4.8	4.8
MPW1KCIS	-4.3	4.3	4.8	-4.2	4.2	4.4	4.3
MPWKCIS1K	-14.9	14.9	18.0	-13.6	13.6	15.4	14.3
PBE1KCIS	-6.4	6.4	8.0	-5.5	5.5	5.9	6.0
TPSSh	-1.4	1.7	2.2	-1.3	1.3	1.5	1.5
TPSS1KCIS	-3.8	3.8	4.4	-3.3	3.3	3.5	3.6
average	*-6.5*	*6.6*		*-5.7*	*5.7*		*6.2*

Table 10: Atomization energies (kcal/mol) for Cr_2, Cu_2, V_2, and Zr_2 (TMAE4/05): The mean signed errors (MSEs), mean unsigned errors (MUEs), root-mean-square errors (RMSEs), and the average mean unsigned errors (AMUEs)

	MSE	MUE	RMSE	MSE	MUE	RMSE	AMUE[a]
	DZQ			TZQ			
HF	-52.4	52.4	55.4	-52.6	52.6	55.4	52.5
LSDA							
SVWN3	26.9	26.9	28.7	37.4	37.4	40.0	32.2
SPWL	23.0	23.0	24.8	32.9	32.9	35.3	28.0
average	*25.0*	*25.0*		*35.2*	*35.2*		*30.1*
GGA							
BLYP	-0.8	2.0	2.1	6.7	7.1	9.0	4.5
BP86	1.2	5.6	6.5	8.0	8.0	10.1	6.8
BPBE	-7.6	8.0	11.0	-2.4	4.7	6.3	6.3
BPW91	-7.5	7.9	10.8	-2.4	4.6	6.2	6.2
G96LYP	-5.7	5.7	7.7	1.6	3.9	4.4	4.8
HCTH	9.5	10.5	12.4	15.4	16.5	18.6	13.5
mPWLYP	2.1	2.4	2.9	9.9	9.9	12.4	6.1
mPWPBE	-4.1	7.4	8.5	1.5	5.1	6.1	6.3
mPWPW91	-4.0	7.3	8.3	1.5	5.0	5.9	6.2
OLYP	-4.5	7.2	7.4	-0.5	7.1	7.7	7.2
PBE	0.4	5.9	6.7	5.4	6.8	8.4	6.3
XLYP	2.0	2.6	2.9	8.3	8.3	10.7	5.4
average	*-1.6*	*6.0*		*4.4*	*7.3*		*6.6*
Hybrid GGA							
B3LYP	-21.5	21.5	28.4	-16.5	16.5	20.4	19.0
B3P86	-18.7	18.7	27.5	-13.9	14.1	20.3	16.4
B3PW91	-25.4	25.4	34.4	-20.7	20.7	27.1	23.1
B97-1	-17.7	18.6	29.7	-8.2	9.0	13.3	13.8
B97-2	-10.1	11.0	17.8	-4.6	5.6	9.7	8.3
B98	-19.7	19.9	31.6	-10.1	10.1	14.9	15.0
BH&HLYP	-35.6	35.6	42.3	-34.3	34.3	40.6	34.9
MPW1K	-32.3	32.3	38.4	-30.8	30.8	37.1	31.5
mPW1PW91	-26.9	26.9	35.5	-25.1	25.1	33.7	26.0
MPW3LYP	-21.8	21.8	30.6	-15.9	15.9	20.6	18.8
O3LYP	-15.4	15.4	20.6	-10.9	12.3	14.9	13.9
PBE1PBE	-25.5	25.5	34.9	-14.4	27.2	33.7	26.4
X3LYP	-21.1	21.1	30.2	-17.3	17.3	21.8	19.2
average	*-22.4*	*22.6*		*-17.1*	*18.4*		*20.5*
Meta GGA							
BB95	3.3	8.0	8.9	11.7	11.7	13.8	9.8
mPWB95	6.4	8.9	9.8	15.6	15.6	17.7	12.2
MPWKCIS	-2.6	5.9	6.7	3.3	5.2	6.3	5.6
PBEKCIS	0.1	4.8	5.3	7.3	7.3	9.5	6.0
TPSSKCIS	-5.2	6.8	8.7	1.5	3.8	4.4	5.3
TPSS	-6.2	8.4	10.9	0.2	3.3	4.4	5.8

VSXC	3.3	4.6	7.9	4.1	6.7	7.9	5.7
average	*-0.1*	*6.7*		*6.2*	*7.7*		*7.2*
			Hybrid Meta GGA				
B1B95	-25.6	25.6	35.0	-21.5	21.5	29.8	23.6
BB1K	-30.0	30.0	37.1	-28.3	28.3	36.0	29.2
MPW1B95	-25.5	25.5	35.0	-22.5	22.5	31.7	24.0
MPW1KCIS	-18.8	18.8	25.5	-14.4	14.4	18.8	16.6
MPWKCIS1K	-32.3	32.3	38.4	-31.0	31.0	37.3	31.6
PBE1KCIS	-24.5	24.5	33.3	-19.6	19.6	25.7	22.0
TPSSh	-16.0	16.0	23.7	-10.5	10.5	14.5	13.2
TPSS1KCIS	-18.3	18.3	25.1	-8.5	8.5	9.9	13.4
average	*-23.9*	*23.9*		*-19.5*	*19.5*		*21.7*

Table 11: Bond lengths (Å) for the dimers in TMBL8/05: The mean signed errors (MSEs), mean unsigned errors (MUEs), root-mean-square errors (RMSEs), and the average mean unsigned errors (AMUEs)

	MSE	MUE	RMSE	MSE	MUE	RMSE	AMUE[a]
	DZQ			TZQ			
HF	0.54	0.57	0.84	0.47	0.51	0.81	0.54
LSDA							
SVWN3	-0.02	0.04	0.05	-0.04	0.05	0.06	0.05
SPWL	-0.01	0.04	0.05	-0.03	0.07	0.31	0.05
average	*-0.01*	*0.04*		*0.02*	*0.06*		*0.05*
GGA							
BLYP	0.11	0.11	0.16	0.03	0.04	0.05	0.08
BP86	0.10	0.10	0.20	0.02	0.03	0.04	0.07
BPBE	0.15	0.15	0.27	0.01	0.03	0.03	0.09
BPW91	0.13	0.13	0.26	0.02	0.03	0.04	0.08
G96LYP	0.11	0.11	0.19	0.03	0.04	0.04	0.07
HCTH	0.16	0.17	0.30	0.14	0.16	0.29	0.16
mPWLYP	0.10	0.10	0.14	0.03	0.04	0.05	0.07
mPWPBE	0.14	0.14	0.25	0.02	0.03	0.03	0.08
mPWPW91	0.13	0.13	0.25	0.02	0.03	0.04	0.08
OLYP	0.16	0.16	0.28	0.11	0.13	0.25	0.14
PBE	0.13	0.13	0.24	0.02	0.03	0.03	0.08
XLYP	0.10	0.10	0.15	0.03	0.04	0.05	0.07
average	*0.13*	*0.13*		*0.04*	*0.05*		*0.09*
hybrid GGA							
B3LYP	0.15	0.17	0.31	0.13	0.15	0.30	0.16
B3P86	0.14	0.16	0.32	0.11	0.15	0.31	0.16
B3PW91	0.16	0.18	0.34	0.13	0.17	0.33	0.17
B97-1	0.12	0.15	0.28	0.15	0.17	0.29	0.16
B97-2	0.12	0.14	0.28	0.13	0.16	0.28	0.15
B98	0.14	0.16	0.29	0.16	0.17	0.30	0.17
BH&HLYP	0.24	0.25	0.40	0.16	0.22	0.37	0.24
MPW1K	0.21	0.24	0.42	0.21	0.25	0.40	0.24
MPW1PW91	0.17	0.19	0.36	0.13	0.18	0.35	0.18
MPW3LYP	0.15	0.17	0.31	0.12	0.15	0.30	0.16
O3LYP	0.16	0.18	0.32	0.13	0.16	0.31	0.17
PBE1PBE	0.16	0.18	0.35	0.13	0.17	0.34	0.18
X3LYP	0.15	0.17	0.31	0.12	0.16	0.30	0.16
average	*0.16*	*0.18*		*0.14*	*0.17*		*0.18*
meta GGA							
BB95	0.07	0.09	0.11	0.00	0.05	0.06	0.07
mPWB95	0.08	0.11	0.15	0.05	0.09	0.11	0.10
mPWKCIS	0.16	0.17	0.26	0.06	0.08	0.10	0.12
PBEKCIS	0.17	0.17	0.25	0.03	0.06	0.07	0.12
TPSSKCIS	0.13	0.14	0.26	0.02	0.05	0.06	0.10
TPSS	0.14	0.15	0.28	0.04	0.07	0.07	0.11

VSXC	0.12	0.13	0.20	0.10	0.13	0.21	0.13
average	*0.12*	*0.14*		*0.04*	*0.08*		*0.11*
			hybrid meta GGA				
B1B95	0.14	0.15	0.33	0.12	0.14	0.33	0.14
BB1K	0.15	0.15	0.36	0.12	0.15	0.35	0.15
MPW1B95	0.15	0.15	0.33	0.13	0.15	0.33	0.15
MPW1KCIS	0.15	0.15	0.32	0.12	0.14	0.31	0.15
MPWKCIS1K	0.16	0.17	0.37	0.14	0.16	0.37	0.16
PBE1KCIS	0.16	0.16	0.33	0.14	0.15	0.33	0.16
TPSSh	0.15	0.16	0.31	0.11	0.12	0.29	0.14
TPSS1KCIS	0.15	0.16	0.32	0.11	0.12	0.30	0.14
average	*0.15*	*0.16*		*0.12*	*0.14*		*0.15*

[a]average of the MUEs with the DZQ and TZQ basis levels.

Table 12: Bond lengths (Å) for Ag_2, CuAg, Cu_2, and Zr_2: The mean signed errors (MSEs), mean unsigned errors (MUEs), root-mean-square errors (RMSEs), and the average mean unsigned errors (AMUEs) for the bond lengths

	MSE	MUE	RMSE	MSE	MUE	RMSE	AMUE[a]
	DZQ			TZQ			
HF	0.48	0.48	0.51	0.16	0.16	0.18	0.32
			LSDA				
SVWN3	-0.02	0.04	0.03	-0.04	0.04	0.04	0.04
SPWL	-0.02	0.03	0.03	-0.03	0.03	0.03	0.03
average	*-0.02*	*0.03*		*-0.04*	*0.04*		*0.04*
			GGA				
BLYP	0.07	0.07	0.08	0.06	0.06	0.06	0.07
BP86	0.04	0.04	0.05	0.03	0.03	0.03	0.04
BPBE	0.05	0.05	0.05	0.03	0.03	0.04	0.04
BPW91	0.05	0.05	0.05	0.04	0.04	0.04	0.04
G96LYP	0.06	0.06	0.07	0.05	0.05	0.05	0.06
HCTH	0.08	0.08	0.08	0.06	0.06	0.07	0.07
mPWLYP	0.07	0.07	0.07	0.06	0.06	0.06	0.07
mPWPBE	0.05	0.05	0.05	0.03	0.03	0.03	0.04
mPWPW91	0.05	0.05	0.05	0.03	0.03	0.04	0.04
OLYP	0.08	0.08	0.08	0.07	0.07	0.08	0.07
PBE	0.05	0.05	0.05	0.04	0.04	0.04	0.04
XLYP	0.07	0.07	0.07	0.06	0.06	0.06	0.07
average	*0.06*	*0.06*		*0.05*	*0.05*		*0.05*
			hybrid GGA				
B3LYP	0.06	0.06	0.06	0.05	0.05	0.06	0.06
B3P86	0.04	0.04	0.04	0.02	0.03	0.04	0.03
B3PW91	0.05	0.05	0.05	0.03	0.04	0.04	0.04
B97-1	0.07	0.07	0.07	0.06	0.06	0.06	0.06
B97-2	0.06	0.06	0.06	0.05	0.05	0.06	0.06
B98	0.06	0.06	0.06	0.05	0.05	0.06	0.06
BH&HLYP	0.07	0.07	0.07	0.06	0.07	0.08	0.07
MPW1K	0.05	0.05	0.05	0.03	0.06	0.06	0.05
MPW1PW91	0.05	0.05	0.05	0.03	0.04	0.05	0.05
MPW3LYP	0.06	0.06	0.06	0.05	0.05	0.06	0.06
O3LYP	0.07	0.07	0.08	0.06	0.07	0.07	0.07
PBE1PBE	0.05	0.05	0.05	0.03	0.05	0.05	0.05
X3LYP	0.06	0.06	0.06	0.05	0.05	0.06	0.06
average	*0.06*	*0.06*		*0.04*	*0.05*		*0.05*
			meta GGA				
BB95	0.06	0.06	0.06	0.04	0.04	0.04	0.05
mPWB95	0.06	0.06	0.06	0.05	0.05	0.05	0.05
mPWKCIS	0.06	0.06	0.06	0.05	0.05	0.05	0.05
PBEKCIS	0.08	0.08	0.08	0.06	0.06	0.07	0.07
TPSSKCIS	0.05	0.05	0.05	0.03	0.03	0.03	0.04
TPSS	0.06	0.06	0.06	0.05	0.05	0.05	0.05

VSXC	0.07	0.07	0.07	0.06	0.06	0.06	0.07
average	*0.06*	*0.06*		*0.05*	*0.05*		*0.05*
			hybrid meta GGA				
B1B95	0.04	0.04	0.04	0.02	0.04	0.04	0.04
BB1K	0.03	0.03	0.04	0.01	0.04	0.04	0.04
MPW1B95	0.05	0.05	0.05	0.04	0.05	0.06	0.05
MPW1KCIS	0.04	0.04	0.04	0.03	0.03	0.04	0.04
MPWKCIS1K	0.05	0.05	0.05	0.04	0.05	0.06	0.05
PBE1KCIS	0.06	0.06	0.06	0.05	0.05	0.06	0.06
TPSSh	0.05	0.05	0.05	0.03	0.03	0.04	0.04
TPSS1KCIS	0.04	0.04	0.04	0.02	0.02	0.02	0.03
average	*0.04*	*0.04*		*0.03*	*0.04*		*0.04*

[a] The AMUE denotes average mean unsigned error and is the average of the MUEs with the DZQ and TZQ basis levels.

Table 13. Mean signed errors (MSEs) and mean unsigned errors (MUEs), in Å, for bond lengths and lattice constants.

		SPWL		PBE		TPSS	
Data	Source	MSE	MUE	MSE	MUE	MSE	MUE
8 metal dimers	Table 11	0.10	0.10	0.08	0.08	0.09	0.11
4 metal dimers	Table 12	0.03	0.03	0.04	0.04	0.05	0.05
4 main group metals	Ref. 97	–0.09	0.09	0.03	0.04	0.05	0.05
4 transition metals	Ref. 97	–0.04	0.04	0.06	0.06	0.03	0.03

Figure Captions

Fig 1. The potential energy curves for Cr_2 computed with BLYP/TZQ (□), MPW1B95/TZQ (○), MPWKCIS/TZQ (×), MPW1KCIS/TZQ (◇), PBE/TZQ (○), and experiment (solid line).

Fig 2. The potential energy curves for Mo_2 computed with BLYP/TZQ (□), MPW1B95/TZQ (○), MPWKCIS/TZQ (×), MPW1KCIS/TZQ (◇), and PBE/TZQ (○).

Fig 3. The potential energy curve for Cr_2 computed with the mPW exchange functional and the KCIS correlation function using the following percentages of Hartree-Fock exchange: $X = 0$ (×), 1 (◇), 2 (□), 3 (+), 4 (△), 5 (○), 6 (✳), 7 (–), and 8 (•), and experiment (solid line).

Fig 4. The optimized bond lengths for the LSDA(△) GGA (×), hybrid GGA (□), meta GGA (◇), and hybrid meta GGA (○) with TZQ basis level and the experimental bond length (line) for Cr_2.

Fig 5. The signed errors in atomization energies for BLYP/DZQ (×), BLYP/TZQ (+), and BLYP/TZQ+*g* (◇) for the dimers in TMAE9/05.

Figure 1

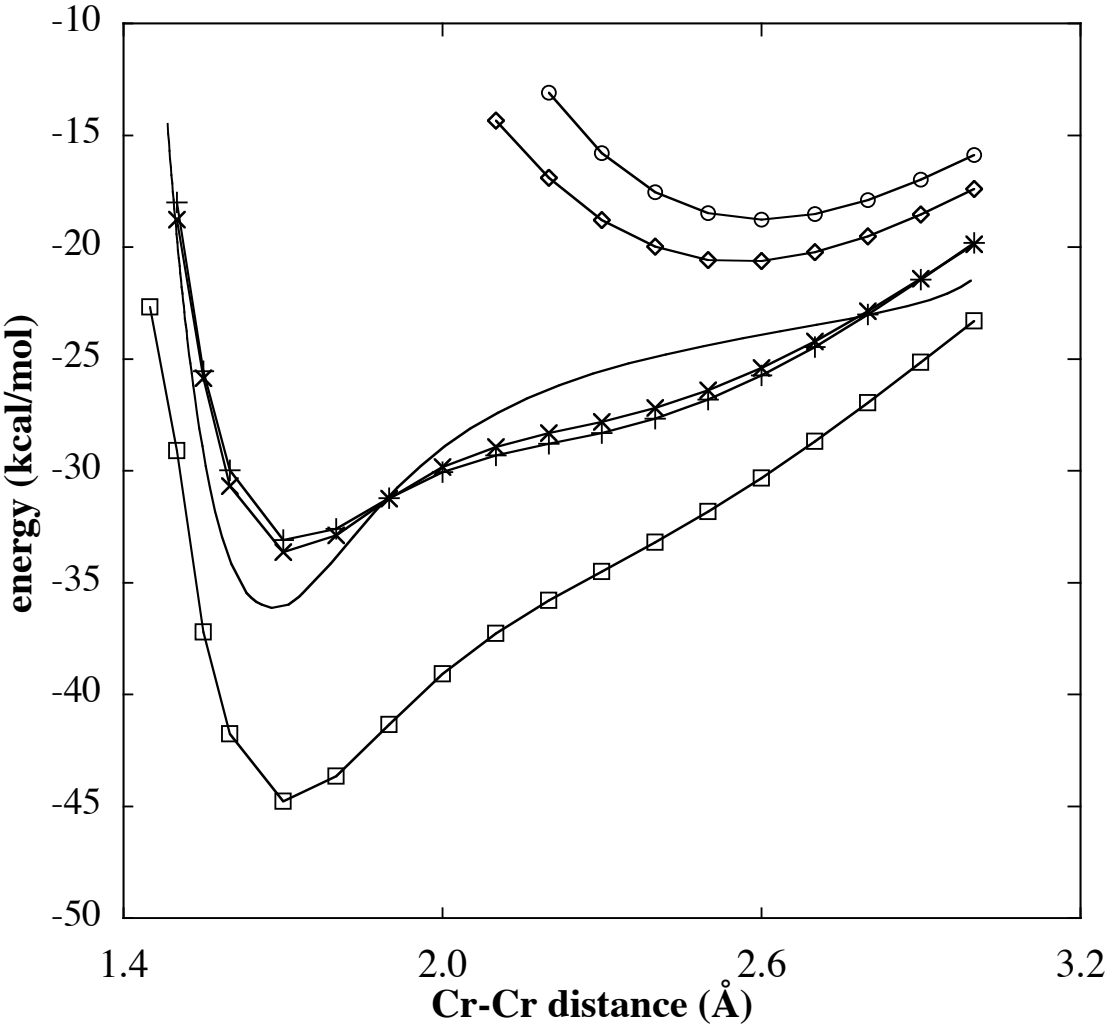
-10
-15
-20
-25
-30
-35
-40
-45
-50
energy (kcal/mol)
1.4
2.0
2.6
3.2
Cr-Cr distance (Å)

Figure 2

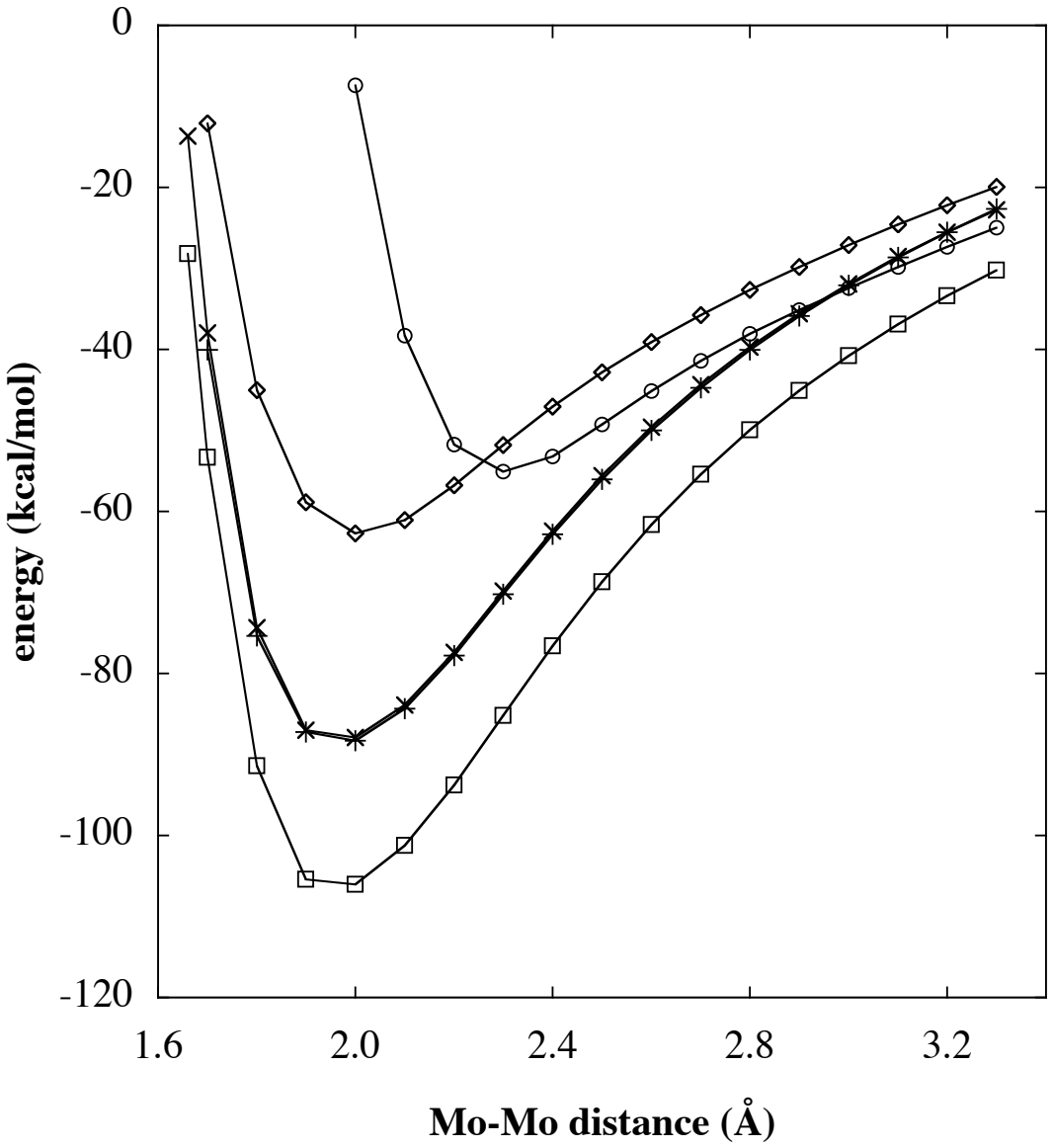
0
-20
-40
-60
-80
-100
-120
energy (kcal/mol)
1.6
2.0
2.4
2.8
3.2
Mo-Mo distance (Å)

Figure 3

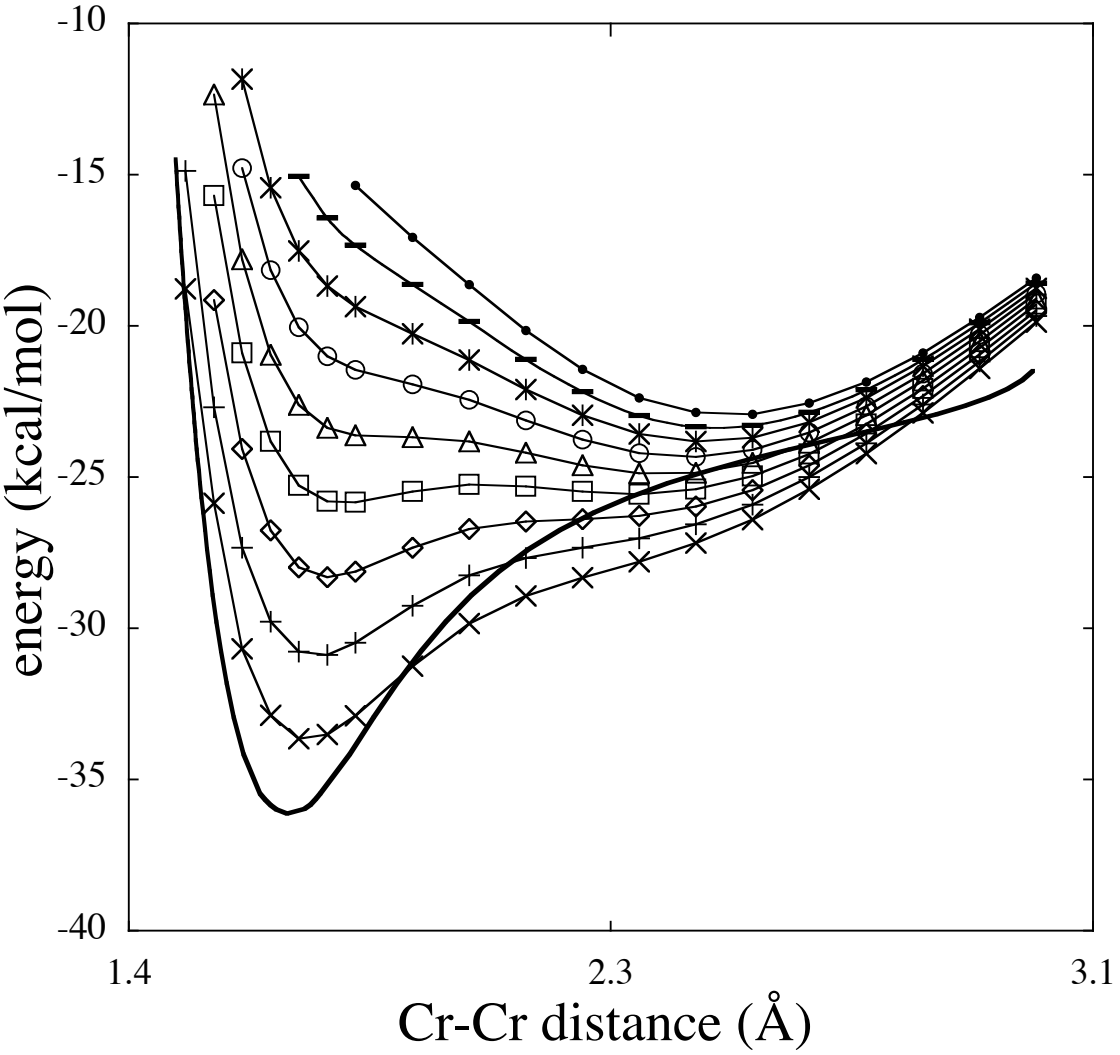

Figure 4

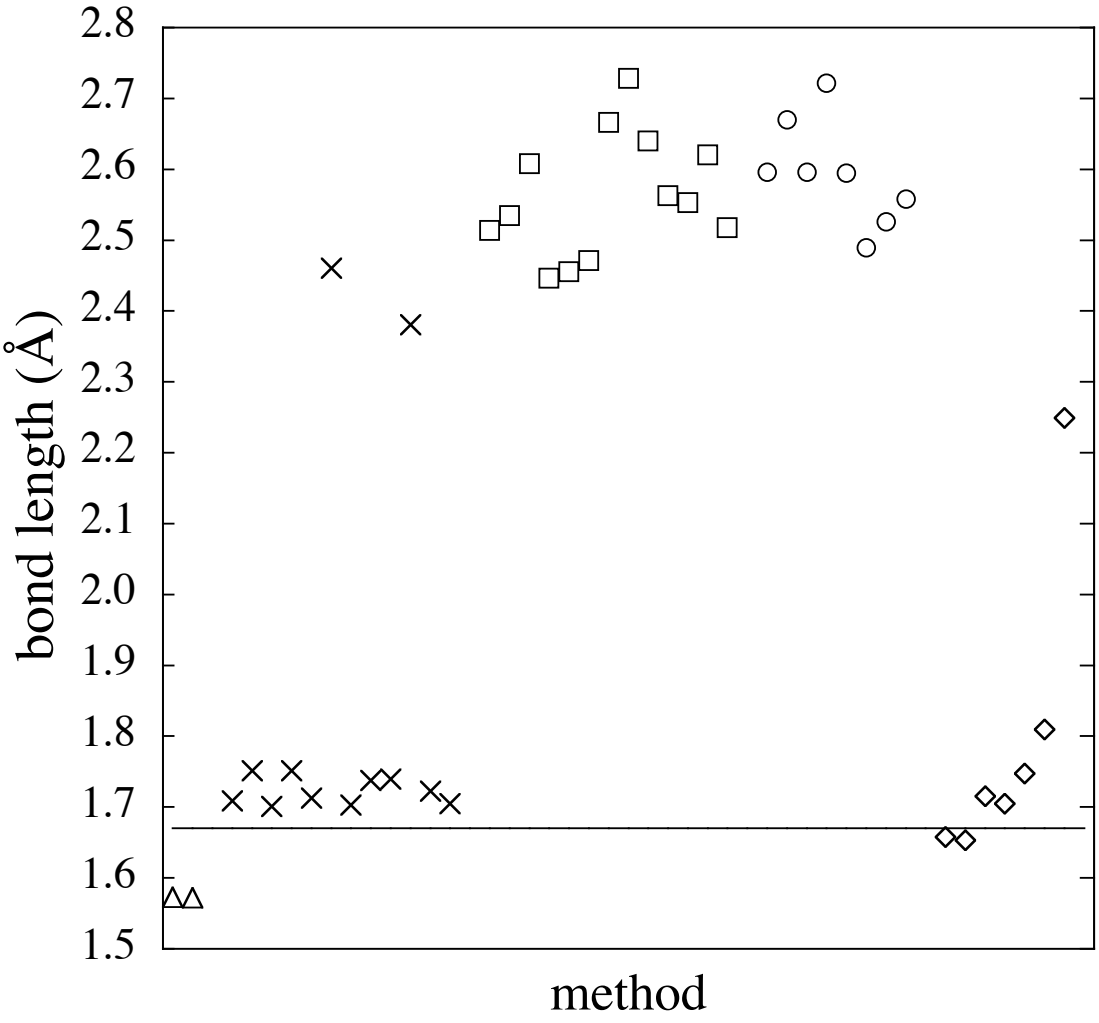

Figure 5

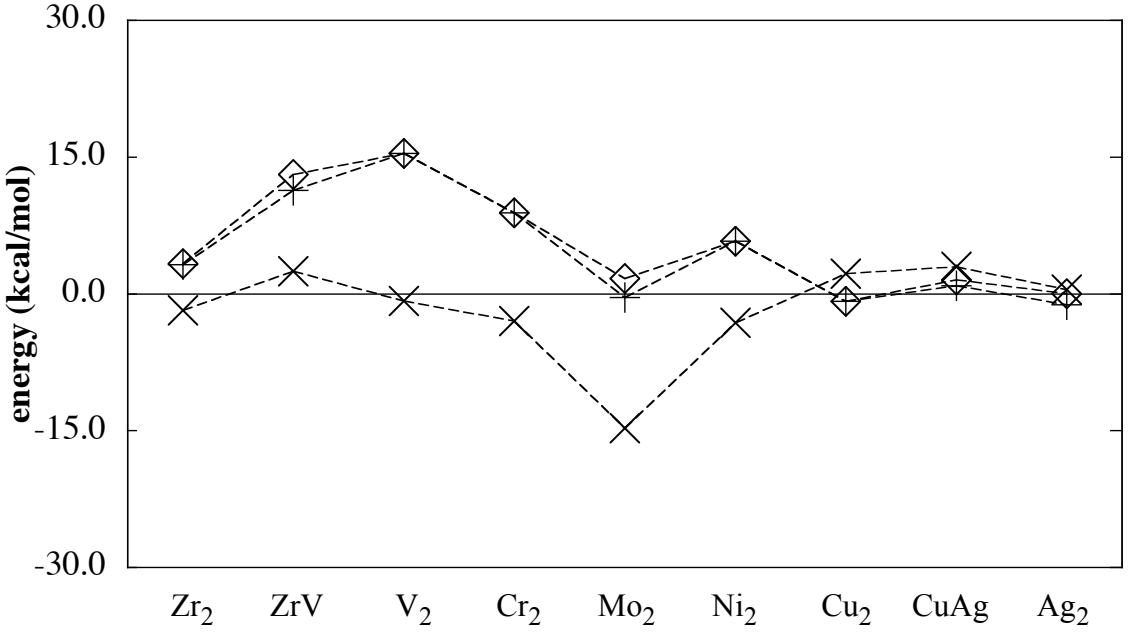
30.0
15.0
0.0
-15.0
-30.0
energy (kcal/mol)
Zr2
ZrV
V2
Cr2
Mo2
Ni2
Cu2
CuAg
Ag2